rine conjugation of hepatic bile acids by *B. wadsworthi*, with direct evidence showing that IL-10-deficient mice fed a low-fat diet containing taurocholic acid, but not glycocholic acid, developed colitis. This paper was the first demonstration that a specific Western-style diet containing high amounts of certain saturated fats enhanced the development of colitis in mice via a specific molecule, taurocholic acid.

JAPANESE AND KOREAN FOODS ARE RECOMMENDED FOR IBD PATIENTS

Prebiotic evidence

Despite findings in many animal models of colitis, decreased dietary fiber intake is not definitely associated with IBD development. However, in daily clinical practice, some dieticians may instruct IBD patients to avoid dietary fiber, at least during the inflammatory stages, because fiber may stimulate the intestinal mucosa. Patients with CD and severe stenosis of the intestine may also be advised to avoid dietary fiber because of the possible intestinal obstruction. However, in our clinical practice at Keio University Hospital, which treats > 2,000 IBD patients, we have explained recently published findings on the roles of dietary fiber in the suppression of inflammation to patients, and have recommended that these patients consume more dietary fiber, including fruits, vegetables, seaweeds, dried mushrooms and dried Japanese radishes. Modern Japanese individuals prefer hulled white rice to unthreshed brownish rice, which contains rice bran with a glucan fiber-rich component. Additionally, wheat bran is discarded when making soft white bread. Because the modern Japanese lifestyle may not allow individuals to eat proper meals, we recommend that IBD patients consume boiled rice together with an individually acceptable proportion of barley, which was a historical part of the normal Japanese lifestyle. The goal is to gradually increase the intake of properly balanced soluble and insoluble dietary fiber every month or year, because both the proportion and absolute numbers of fermented probiotics strains are reduced in the intestines of IBD patients [57]. A gradual increase in fermenters may allow patients to handle increased amounts of dietary fiber. The quantity of fermenters present in the intestines of these patients at the beginning of probiotic treatment may be insufficient to handle an overabundance of dietary fiber, resulting in deleterious outcomes, such as intestinal obstruction.

Probiotic evidence

The intake of foods containing fermented probiotics has decreased in Japan. Traditionally, Japanese have eaten fermented foods, such as fermented pickled vegetables, fermented bean paste, fermented stockfishes, fermented fish sushi, and natto. Fermentation was originally used to preserve foods and protect against putrefactive bacteria, such as pathobionts, prior to the widespread availability of electric refrigerators around 1963. Modern Japanese may avoid eating fermented foods owing to their strong smell. Indeed, modern Japanese, especially younger individuals, prefer light Kimchi, which can be made overnight, rather than sour Kimchi, which requires several months to ferment and produce abundant probiotics (*Lactobacillus*) and SCFAs. Additionally, young Japanese individuals do not like to eat Kusaya, a type of deeply fermented fish similar to Hongeohoe in Korea, both of which have powerful smells.

CONCLUSIONS

Randomized controlled trials have shown evidence for the effectiveness of fecal microbiota transplantation (FMT) in patients with recurrent *Clostridium difficile* infection (CDI) [58], and several case studies have shown the benefit of FMT for patients with IBD [58-60]. FMT may normalize dysbiosis in patients with IBD, but the strategy used in patients with recurrent CDI may have to be modified for patients with IBD. Although the incidence of IBD in developed Asian countries is rapidly increasing, so is the incidence in developed Western countries. Asian societies are at a crossroads between a Western-style and a traditional high-fiber, low-fat, and fermenter-rich diet. Clinicians should encourage these traditional foods to promote public welfare.

Conflict of interest

No potential conflict of interest relevant to this article was reported.

http://dx.doi.org/10.3904/kjim.2014.29.4.409

Acknowledgments

We thank A. Hayashi at Keio University School of Medicine for critical comments.

REFERENCES

1. Japan Intractable Diseases Information Center. Annual report 2012 from Japan Intractable Diseases Information Center [Internet]. [place unknown]: Japan Intractable Diseases Information Center, 2014 [cited 2014 May 1]. Available from: http://www.nanbyou.or.jp/entry/1356.
2. Asakura H, Suzuki K, Kitahora T, Morizane T. Is there a link between food and intestinal microbes and the occurrence of Crohn's disease and ulcerative colitis? J Gastroenterol Hepatol 2008;23:1794-1801.
3. Danese S, Fiocchi C. Ulcerative colitis. N Engl J Med 2011;365:1713-1725.
4. Molodecky NA, Soon IS, Rabi DM, et al. Increasing incidence and prevalence of the inflammatory bowel diseases with time, based on systematic review. Gastroenterology 2012;142:46-54.
5. Jostins L, Ripke S, Weersma RK, et al. Host-microbe interactions have shaped the genetic architecture of inflammatory bowel disease. Nature 2012;491:119-124.
6. Aujnarain A, Mack DR, Benchimol EI. The role of the environment in the development of pediatric inflammatory bowel disease. Curr Gastroenterol Rep 2013;15:326.
7. Leone V, Chang EB, Devkota S. Diet, microbes, and host genetics: the perfect storm in inflammatory bowel diseases. J Gastroenterol 2013;48:315-321.
8. Goldsmith JR, Sartor RB. The role of diet on intestinal microbiota metabolism: downstream impacts on host immune function and health, and therapeutic implications. J Gastroenterol 2014;49:785-798.
9. Kostic AD, Xavier RJ, Gevers D. The microbiome in inflammatory bowel disease: current status and the future ahead. Gastroenterology 2014;146:1489-1499.
10. Manichanh C, Borruel N, Casellas F, Guarner F. The gut microbiota in IBD. Nat Rev Gastroenterol Hepatol 2012;9:599-608.
11. Kaur N, Chen CC, Luther J, Kao JY. Intestinal dysbiosis in inflammatory bowel disease. Gut Microbes 2011;2:211-216.
12. Knights D, Lassen KG, Xavier RJ. Advances in inflammatory bowel disease pathogenesis: linking host genetics and the microbiome. Gut 2013;62:1505-1510.
13. Neuman MG, Nanau RM. Inflammatory bowel disease: role of diet, microbiota, life style. Transl Res 2012;160:29-44.
14. Wu GD, Chen J, Hoffmann C, et al. Linking long-term dietary patterns with gut microbial enterotypes. Science 2011;334:105-108.
15. Sommer F, Backhed F. The gut microbiota: masters of host development and physiology. Nat Rev Microbiol 2013;11:227-238.
16. Cho I, Yamanishi S, Cox L, et al. Antibiotics in early life alter the murine colonic microbiome and adiposity. Nature 2012;488:621-626.
17. Ivanov, II, Honda K. Intestinal commensal microbes as immune modulators. Cell Host Microbe 2012;12:496-508.
18. Human Microbiome Project Consortium. A framework for human microbiome research. Nature 2012;486:215-221.
19. Blaser M, Bork P, Fraser C, Knight R, Wang J. The microbiome explored: recent insights and future challenges. Nat Rev Microbiol 2013;11:213-217.
20. Blumberg R, Powrie F. Microbiota, disease, and back to health: a metastable journey. Sci Transl Med 2012;4:137rv137.
21. Spor A, Koren O, Ley R. Unravelling the effects of the environment and host genotype on the gut microbiome. Nat Rev Microbiol 2011;9:279-290.
22. Clemente JC, Ursell LK, Parfrey LW, Knight R. The impact of the gut microbiota on human health: an integrative view. Cell 2012;148:1258-1270.
23. Kamada N, Seo SU, Chen GY, Nunez G. Role of the gut microbiota in immunity and inflammatory disease. Nat Rev Immunol 2013;13:321-335.
24. Tyler AD, Smith MI, Silverberg MS. Analyzing the human microbiome: a "how to" guide for physicians. Am J Gastroenterol 2014 Apr 22 [Epub]. http://dx.doi.org/10.1038/ajg.2014.73.
25. Cox MJ, Cookson WO, Moffatt MF. Sequencing the human microbiome in health and disease. Hum Mol Genet 2013;22(R1):R88-R94.
26. McCarthy JJ, McLeod HL, Ginsburg GS. Genomic medicine: a decade of successes, challenges, and opportunities. Sci Transl Med 2013;5:189sr184.
27. Weinstock GM. Genomic approaches to studying the

human microbiota. Nature 2012;489:250-256.
28. Sweeney TE, Morton JM. The human gut microbiome: a review of the effect of obesity and surgically induced weight loss. JAMA Surg 2013;148:563-569.
29. Cho I, Blaser MJ. The human microbiome: at the interface of health and disease. Nat Rev Genet 2012;13:260-270.
30. Round JL, Mazmanian SK. The gut microbiota shapes intestinal immune responses during health and disease. Nat Rev Immunol 2009;9:313-323.
31. Collins SM, Surette M, Bercik P. The interplay between the intestinal microbiota and the brain. Nat Rev Microbiol 2012;10:735-742.
32. Simren M, Barbara G, Flint HJ, et al. Intestinal microbiota in functional bowel disorders: a Rome foundation report. Gut 2013;62:159-176.
33. Power SE, O'Toole PW, Stanton C, Ross RP, Fitzgerald GF. Intestinal microbiota, diet and health. Br J Nutr 2014;111:387-402.
34. Walsh CJ, Guinane CM, O'Toole PW, Cotter PD. Beneficial modulation of the gut microbiota. FEBS Lett 2014 Mar 26 [Epub]. http://dx.doi.org/10.1016/j.febslet.2014.03.035.
35. Le Chatelier E, Nielsen T, Qin J, et al. Richness of human gut microbiome correlates with metabolic markers. Nature 2013;500:541-546.
36. Holmes E, Li JV, Marchesi JR, Nicholson JK. Gut microbiota composition and activity in relation to host metabolic phenotype and disease risk. Cell Metab 2012;16:559-564.
37. Nicholson JK, Holmes E, Kinross J, et al. Host-gut microbiota metabolic interactions. Science 2012;336:1262-1267.
38. De Filippo C, Cavalieri D, Di Paola M, et al. Impact of diet in shaping gut microbiota revealed by a comparative study in children from Europe and rural Africa. Proc Natl Acad Sci U S A 2010;107:14691-14696.
39. Yatsunenko T, Rey FE, Manary MJ, et al. Human gut microbiome viewed across age and geography. Nature 2012;486:222-227.
40. D'Haens GR, Sartor RB, Silverberg MS, Petersson J, Rutgeerts P. Future directions in inflammatory bowel disease management. J Crohns Colitis 2014 Apr 14 [Epub]. http://dx.doi.org/10.1016/j.crohns.2014.02.025.
41. Richman E, Rhodes JM. Review article: evidence-based dietary advice for patients with inflammatory bowel disease. Aliment Pharmacol Ther 2013;38:1156-1171.
42. Guarner F. Hygiene, microbial diversity and immune regulation. Curr Opin Gastroenterol 2007;23:667-672.
43. Spooren CE, Pierik MJ, Zeegers MP, Feskens EJ, Masclee AA, Jonkers DM. Review article: the association of diet with onset and relapse in patients with inflammatory bowel disease. Aliment Pharmacol Ther 2013;38:1172-1187.
44. Hou JK, Lee D, Lewis J. Diet and inflammatory bowel disease: review of patient-targeted recommendations. Clin Gastroenterol Hepatol 2013 Oct 6 [Epub]. http://dx.doi.org/10.1016/j.cgh.2013.09.063.
45. Ananthakrishnan AN, Khalili H, Konijeti GG, et al. A prospective study of long-term intake of dietary fiber and risk of Crohn's disease and ulcerative colitis. Gastroenterology 2013;145:970-977.
46. Devkota S, Chang EB. Nutrition, microbiomes, and intestinal inflammation. Curr Opin Gastroenterol 2013;29:603-607.
47. Veldhoen M, Brucklacher-Waldert V. Dietary influences on intestinal immunity. Nat Rev Immunol 2012;12:696-708.
48. Garrett WS, Lord GM, Punit S, et al. Communicable ulcerative colitis induced by T-bet deficiency in the innate immune system. Cell 2007;131:33-45.
49. Turnbaugh PJ, Ley RE, Mahowald MA, Magrini V, Mardis ER, Gordon JI. An obesity-associated gut microbiome with increased capacity for energy harvest. Nature 2006;444:1027-1031.
50. Atarashi K, Tanoue T, Shima T, et al. Induction of colonic regulatory T cells by indigenous Clostridium species. Science 2011;331:337-341.
51. Atarashi K, Tanoue T, Oshima K, et al. Treg induction by a rationally selected mixture of Clostridia strains from the human microbiota. Nature 2013;500:232-236.
52. Furusawa Y, Obata Y, Fukuda S, et al. Commensal microbe-derived butyrate induces the differentiation of colonic regulatory T cells. Nature 2013;504:446-450.
53. Arpaia N, Campbell C, Fan X, et al. Metabolites produced by commensal bacteria promote peripheral regulatory T-cell generation. Nature 2013;504:451-455.
54. Smith PM, Howitt MR, Panikov N, et al. The microbial metabolites, short-chain fatty acids, regulate colonic Treg cell homeostasis. Science 2013;341:569-573.
55. Hayashi A, Sato T, Kamada N, et al. A single strain of Clostridium butyricum induces intestinal IL-10-pro-

http://dx.doi.org/10.3904/kjim.2014.29.4.409

ducing macrophages to suppress acute experimental colitis in mice. Cell Host Microbe 2013;13:711-722.
56. Devkota S, Wang Y, Musch MW, et al. Dietary-fat-induced taurocholic acid promotes pathobiont expansion and colitis in Il10-/- mice. Nature 2012;487:104-108.
57. Takaishi H, Matsuki T, Nakazawa A, et al. Imbalance in intestinal microflora constitution could be involved in the pathogenesis of inflammatory bowel disease. Int J Med Microbiol 2008;298:463-472.
58. van Nood E, Vrieze A, Nieuwdorp M, et al. Duodenal infusion of donor feces for recurrent Clostridium difficile. N Engl J Med 2013;368:407-415.
59. Kahn SA, Vachon A, Rodriquez D, et al. Patient perceptions of fecal microbiota transplantation for ulcerative colitis. Inflamm Bowel Dis 2013;19:1506-1513.
60. Smits LP, Bouter KE, de Vos WM, Borody TJ, Nieuwdorp M. Therapeutic potential of fecal microbiota transplantation. Gastroenterology 2013;145:946-953.

PLOS ONE

Macrophages and Dendritic Cells Emerge in the Liver during Intestinal Inflammation and Predispose the Liver to Inflammation

Yohei Mikami[1,2], Shinta Mizuno[1], Nobuhiro Nakamoto[1], Atsushi Hayashi[1,3], Tomohisa Sujino[1], Toshiro Sato[1], Nobuhiko Kamada[4], Katsuyoshi Matsuoka[1], Tadakazu Hisamatsu[1], Hirotoshi Ebinuma[1], Toshifumi Hibi[1], Akihiko Yoshimura[2]*, Takanori Kanai[1]*

1 Division of Gastroenterology and Hepatology, Department of Internal Medicine, Keio University School of Medicine, Tokyo, Japan, **2** Department of Microbiology and Immunology, Keio University School of Medicine, Tokyo, Japan, **3** Research Laboratory, Miyarisan Pharmaceutical, Tokyo, Japan, **4** Department of Pathology and Comprehensive Cancer Center, University of Michigan Medical School, Ann Arbor, Michigan, United States of America

Abstract

The liver is a physiological site of immune tolerance, the breakdown of which induces immunity. Liver antigen-presenting cells may be involved in both immune tolerance and activation. Although inflammatory diseases of the liver are frequently associated with inflammatory bowel diseases, the underlying immunological mechanisms remain to be elucidated. Here we report two murine models of inflammatory bowel disease: RAG-2$^{-/-}$ mice adoptively transferred with CD4^{+}CD45RB^{high} T cells; and IL-10$^{-/-}$ mice, accompanied by the infiltration of mononuclear cells in the liver. Notably, CD11b^{-}CD11c^{low}PDCA-1^{+} plasmacytoid dendritic cells (DCs) abundantly residing in the liver of normal wild-type mice disappeared in colitic CD4^{+}CD45RB^{high} T cell-transferred RAG-2$^{-/-}$ mice and IL-10$^{-/-}$ mice in parallel with the emergence of macrophages (Mφs) and conventional DCs (cDCs). Furthermore, liver Mφ/cDCs emerging during intestinal inflammation not only promote the proliferation of naïve CD4^{+} T cells, but also instruct them to differentiate into IFN-γ-producing Th1 cells *in vitro*. The emergence of pathological Mφ/cDCs in the liver also occurred in a model of acute dextran sulfate sodium (DSS)-induced colitis under specific pathogen-free conditions, but was canceled in germ-free conditions. Last, the Mφ/cDCs that emerged in acute DSS colitis significantly exacerbated Fas-mediated hepatitis. Collectively, intestinal inflammation skews the composition of antigen-presenting cells in the liver through signaling from commensal bacteria and predisposes the liver to inflammation.

Citation: Mikami Y, Mizuno S, Nakamoto N, Hayashi A, Sujino T, et al. (2014) Macrophages and Dendritic Cells Emerge in the Liver during Intestinal Inflammation and Predispose the Liver to Inflammation. PLoS ONE 9(1): e84619. doi:10.1371/journal.pone.0084619

Editor: David L. Boone, University of Chicago, United States of America

Received October 11, 2013; **Accepted** November 25, 2013; **Published** January 2, 2014

Copyright: © 2014 Mikami et al. This is an open-access article distributed under the terms of the Creative Commons Attribution License, which permits unrestricted use, distribution, and reproduction in any medium, provided the original author and source are credited.

Funding: This study was supported in part by Grants-in-Aid for Scientific Research [21390233], Scientific Research on Priority Areas [22021038] from the Japanese Ministry of Education, Culture, Sports, Science and Technology; a Grant-in-Aid for Young Scientists [22790667] from the Japanese Ministry of Health, Labour and Welfare; Health and Labour Sciences Research Grants for research on intractable diseases from the Japanese MIKAMI ET AL Ministry of Health, Labour and Welfare; a Keio University Grant-in-Aid for Encouragement of Young Medical Scientists. The funders had no role in study design, data collection and analysis, decision to publish, or preparation of the manuscript.

Competing Interests: AH is employed by a commercial company, Miyarisan Pharmaceutical. This does not alter the authors' adherence to all the PLOS ONE policies on sharing data and materials.

* E-mail: takagast@z2.keio.jp (TK); yoshimura@a6.keio.jp (AY)

Introduction

Patients with inflammatory bowel diseases (IBD) are susceptible to developing extraintestinal disorders in the joints, eyes, skin, or liver [1]. For example, primary sclerosing cholangitis (PSC) has been diagnosed in 3.7% of patients with ulcerative colitis [2] and in 3.4% of those with Crohn's disease [3]. The liver and the biliary system are the usual sites for extraintestinal lesions, despite being located between systemic and portal circulations. The portal vein contains a large amount of gut-derived products, such as short-chain fatty acids and microbe-associated molecular patterns (MAMPs) [4]. Although MAMPs, such as LPS from gram-negative commensal bacteria, act as a strong stimulants for antigen-presenting cells (APCs) [5], the liver has been shown to be an immunologically tolerant organ [6,7]. The portal venous tolerance system is regulated by various immune compartments which contain natural killer (NK) cell, natural killer T (NKT) cell, and regulatory T cells, macrophages (Mφ) such as Kupffer cells, and dendritic cells (DCs) [8]. Recent studies have shown that plasmacytoid DCs (pDCs), a subgroup of resident DCs, induce anergy or rapid depletion of antigen-specific T cells in the liver via a CD4^{+} T cell-independent mechanism [9,10]. These findings suggest that regulation and dysregulation of APCs in the liver contribute to liver tolerance and inflammation, respectively. However, the mechanisms of immune regulation and dysregulation in human IBD and experimental colitis models are not yet fully understood. A few studies have focused on the role of gut microbiota and MAMPs in promoting high-fat induced steatohepatitis [11], however, mechanism of immunological dysregulation in the liver during colitis still remains to be elucidated.

Our group has previously reported that increased numbers of Mφs and conventional DCs (cDCs) in experimental colitis models [12] and human IBD [13] have pro-inflammatory characteristics through excess production of IL-12 and IL-23 in response to

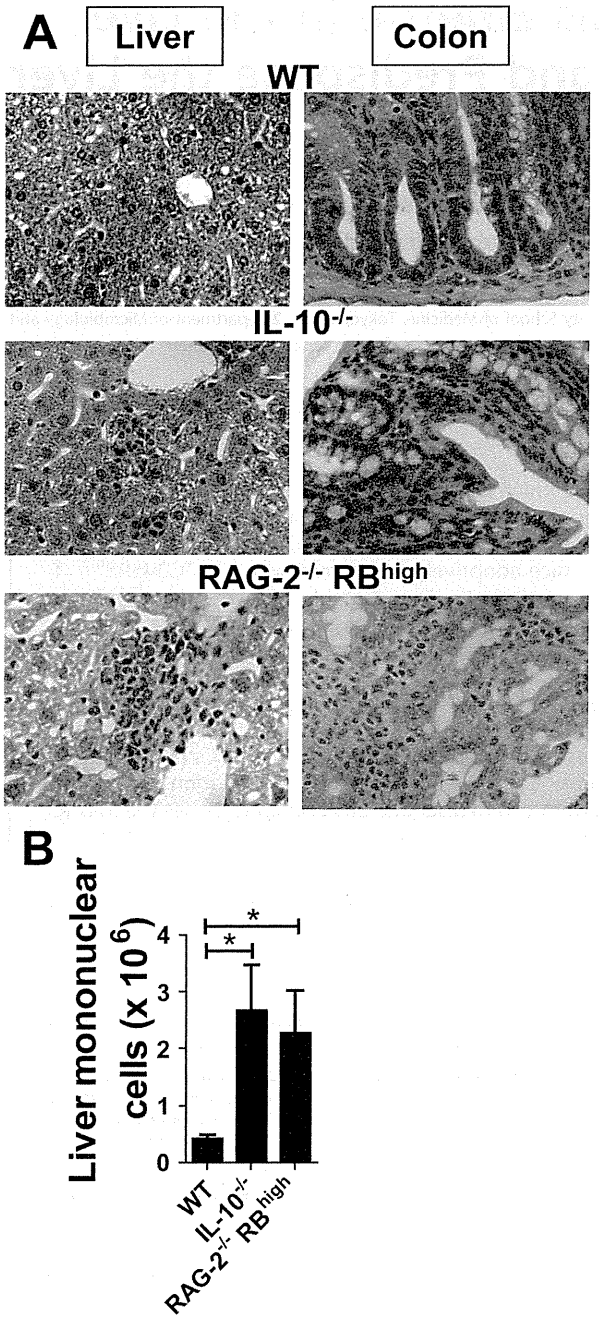

Figure 1. Accumulation of mononuclear cells in the liver develops in chronic colitis models. (**A**) H&E specimens of the liver (left) and colon (right) derived from WT, IL-$10^{-/-}$ mice, and RAG-$2^{-/-}$ RB^{high} mice. Magnification: ×100 (left) and ×400 (right). (**B**) Absolute number of hepatic mononuclear cells. FACS data are representative of three independent experiments. Values are expressed as means ± SEM for each group. WT ($n=5$), IL-$10^{-/-}$ mice ($n=7$) and RAG-$2^{-/-}$ RB^{high} mice ($n=4$). *$P<0.05$.
doi:10.1371/journal.pone.0084619.g001

bacteria. This leads to the development of Th1 immunity in inflamed intestinal mucosa. More recently, we demonstrated that migrating macrophages contribute to the induction of acute liver inflammation in murine hepatitis models [14].

To clarify hepatic immunological regulation under colitic conditions, we used three murine IBD models: (1) RAG-$2^{-/-}$ mice adoptively transferred with splenic $CD4^+CD45RB^{high}$ T cells from wild-type (WT) mice [15]; (2) an acute dextran sulfate sodium (DSS)-induced colitis model [16]; and (3) IL-$10^{-/-}$ mice [17] that spontaneously develop chronic IBD-like colitis.

Materials and Methods

Mice

WT C57BL/6J mice (8–12 weeks old) were purchased from Japan Clea (Tokyo, Japan). C57BL/6-Ly5.1 mice and RAG-$2^{-/-}$ mice were obtained from Taconic Laboratory (Hudson, NY, USA) and the Central Laboratories for Experimental Animals (Kawasaki, Japan), respectively. IL-$10^{-/-}$ mice were purchased from Jackson Laboratories (Bar Harbor, Maine, USA). Recipient RAG-$2^{-/-}$ mice were used when they were 6 or 14 weeks old. Colitic IL-$10^{-/-}$ mice were used when they were 20 weeks old. Germ-free (GF) C57BL/6-Ly5.2 mice (8 weeks old) were purchased from Sankyo Laboratories (Tokyo, Japan). GF mice were maintained in vinyl isolators within the gnotobiotic facility of the Miyarisan pharmaceutical company (Tokyo, Japan).

All experiments were approved by the Committee on the Ethics of Animal Experiments of Keio University School of Medicine, and conducted in accordance with institutional guidelines and Home Office regulations. [No. 24-026-1].

Adoptive Transfer Studies

For adoptive transfer, $CD4^+$ T cells were isolated from spleen cells of C57BL/6-Ly5.1 mice using the anti-CD4 (L3T4)-MACS system (Miltenyi Biotec, Auburn, CA, USA) according to the manufacturer's instructions. Enriched $CD4^+$ T cells (96–97% pure) were labeled with PE-conjugated anti-mouse CD4 (RM4-5; BD bioscience, San Diego, CA, USA) and FITC-conjugated anti-CD45RB (16A; BD bioscience). $CD4^+CD45RB^{high}$ cells were purified (>98.0%) using a FACS Aria (Becton Dickinson Co.). RAG-$2^{-/-}$ mice (6 weeks old) were injected i.p. with 3×10^5 $CD4^+CD45RB^{high}$ T cells. At 6 weeks post-transfer, these mice developed a wasting disease and colitis as previously reported [15].

For adoptive retransfer, lamina propria (LP) $CD4^+$ T cells were isolated from colon LP mononuclear cells of RAG-$2^{-/-}$ RB^{high} mice using the anti-CD4 (L3T4)-MACS system. Isolated LP $CD4^+$ T cells were injected i.p. into RAG-$2^{-/-}$ mice (RAG-$2^{-/-}$ LP $CD4^+$ mice). Mice were maintained under specific pathogen-free (SPF) conditions in the Animal Care Facility of Keio University.

DSS-induced Colitis Model

Mice were treated under SPF conditions with 2% DSS (MW 50 kDa; Ensuiko Sugar Refining Co., Yokohama, Japan) in drinking water for 7 days (>4 mice per group). Mice were treated under GF conditions with 1% DSS in drinking water for 7 days followed with regular drinking water for 3 days (>4 mice per group).

Animal Models of Liver Injury

Concanavalin A (Con A, type IV) was purchased from Sigma-Aldrich (St. Louis, MO, USA). Intravenous injections of Con A (20 mg/kg) were administered into the tail vein of animals 10 h before examination. The Fas-activating antibody Jo2 (0.3 mg/kg of body weight; BD bioscience) was injected i.p. and mice were sacrificed 6 h later [18,19].

Preparation of Liver Mononuclear Cells

Liver mononuclear cells were separated from the liver as previously described [20]. Livers were perfused through the portal vein with PBS, then minced and passed through a 100 μm nylon mesh. The filtrate was centrifuged at 50×*g* for 1 min, and the

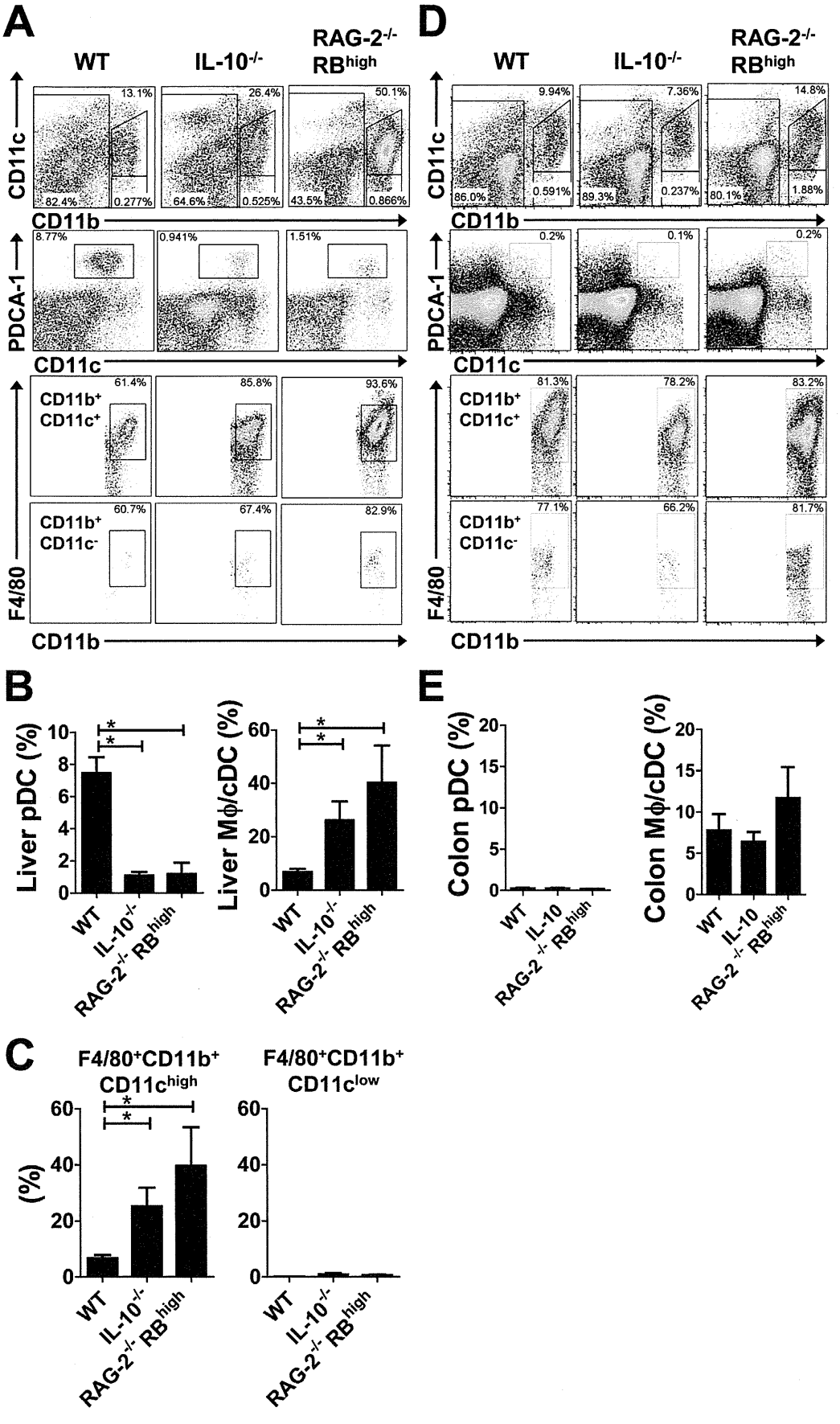
A
WT
IL-10-/-
RAG-2-/- RBhigh
CD11c
CD11b
13.1%
82.4%
0.277%
26.4%
64.6%
0.525%
50.1%
43.5%
0.866%
PDCA-1
CD11c
8.77%
0.941%
1.51%
CD11b+ CD11c+
61.4%
85.8%
93.6%
CD11b+ CD11c-
60.7%
67.4%
82.9%
F4/80
CD11b
D
WT
IL-10-/-
RAG-2-/- RBhigh
CD11c
CD11b
9.94%
86.0%
0.591%
7.36%
89.3%
0.237%
14.8%
80.1%
1.88%
PDCA-1
CD11c
0.2%
0.1%
0.2%
CD11b+ CD11c+
81.3%
78.2%
83.2%
CD11b+ CD11c-
77.1%
66.2%
81.7%
F4/80
CD11b
B
Liver pDC (%)
Liver Mϕ/cDC (%)
WT
IL-10-/-
RAG-2-/- RBhigh
E
Colon pDC (%)
Colon Mϕ/cDC (%)
WT
IL-10
RAG-2-/- RBhigh
C
F4/80+CD11b+ CD11chigh
F4/80+CD11b+ CD11clow
(%)
WT
IL-10-/-
RAG-2-/- RBhigh

Figure 2. Chronic intestinal inflammation was associated with reciprocal changes in the balance of APCs. (**A**) Flow cytometry results related to mononuclear cells isolated from the livers of WT (left column), IL-10$^{-/-}$ (middle), and RAG-2$^{-/-}$ RB^{high} (right) mice. Dead cells were excluded with 7AAD staining, followed by proper use of a FSC/SSC gate. CD11b^{-}, CD11b^{+}CD11c^{high}, and CD11b^{+}CD11c^{low} cells were gated from the cells shown in the first row. CD11b^{-} cells are shown in the second row and PDCA-1^{+}CD11b^{-}CD11c^{int} cells were analyzed. The expression of F4/80 in CD11b^{+}CD11c^{high} cells and CD11b^{+}CD11c^{low} cells are analyzed in the third row and the fourth row. (**B**) Proportion of PDCA-1^{+}CD11b^{-}CD11c^{int} pDCs and F4/80^{+}CD11b^{+} Mφ/cDCs among whole mononuclear cells. (**C**) Proportion of F4/80^{+} CD11b^{+}CD11c^{high} Mφ/cDCs and F4/80^{+} CD11b^{+}CD11c^{low} Mφ/cDCs among whole mononuclear cells. (**D**) Flow cytometry analysis of mononuclear cells isolated from the colons of WT (left column), IL-10$^{-/-}$ (middle), and RAG-2$^{-/-}$ RB^{high} (right) mice. (**E**) Proportion of PDCA-1^{+}CD11b^{-}CD11c^{+} pDCs and F4/80^{+}CD11b^{+}CD11c^{-} Mφ/cDCs among whole mononuclear cells. FACS data are representative of three independent experiments expressed as means ± SEM for each group. WT ($n=4$), IL-10$^{-/-}$ ($n=4$) and RAG-2$^{-/-}$ RB^{high} ($n=3$) mice. *$P<0.05$.
doi:10.1371/journal.pone.0084619.g002

supernatant washed once. Cells were suspended in Histopaque solution (Sigma-Aldrich) and overlaid on HBSS. After centrifugation (780×*g* for 20 min), cells were collected from the upper phase.

Preparation of LP Mononuclear Cells

Cell isolation was performed as previously described [21]. Dissected colon mucosa was incubated with Ca^{2+}, Mg^{2+}-free HBSS containing 1 mM DTT (Sigma-Aldrich) and 5 μM EDTA (Gibco) for 30 min, then treated with 3 mg/ml collagenase (Roche Diagnostics GmbH, Germany) and 0.01% DNase (Worthington Biomedical Co., Freehold, NJ, USA) for 1 h. Cells were pelleted twice through a 40% isotonic Percoll solution and then subjected to Ficoll-Hypaque density gradient centrifugation (40%/75%).

Histological Examination

Liver and colon were fixed in 10% formalin and embedded in paraffin. Sections were stained with H&E and then examined. Histological examination of acute colitis was performed as described previously [22]. Briefly, histological activity score was assessed as the sum of three parameters as follows: extent, 0–3 (0, none; 1, mucosa; 2, mucosa and submucosa; 3, transmural); inflammation, 0–3 (0, none; 1, slight; 2, moderate; 3, severe); crypt damage, 0–4 (0, none; 1, basal 1/3 lost; 2, basal 2/3 lost; 3, only surface epithelium intake; 4, entire crypt and epithelium lost). The score of each parameter was multiplied by a factor of 1–4 (1, 0–25%; 2, 26–50%; 3, 51–75%; 4, 76–100%) according to the percentage of epithelial involvement.

Flow Cytometry

After blocking with anti-FcR (CD16/32, BD bioscience) for 20 min, cells were incubated with specific mAbs at 4°C for 30 min. The following mAbs were used: anti-mouse CD3e-APC-Cy7; anti-CD4-PE-Cy7; anti-NK1.1-APC; anti-CD11b-PE-Cy7; anti-CD11cFITC; 7-AAD; anti-PDCA-1-APC; anti-CCR9-PE; anti-IFN-γ-FITC; and anti-IL-17-APC (eBioscience, BD bioscience). Background fluorescence was assessed by staining with irrelevant anti-rat isotypes (BD bioscience). Stained cells were analyzed by flow cytometry (FACS Canto II, Becton Dickinson Co.) and data analyzed using FlowJo software (Tree Star Inc.) [12].

Quantitative RT-PCR (qPCR)

All qPCR assays were performed as described previously [14]. RNA was extracted from LP mononuclear cells using TRIzol reagent (Invitrogen, Carlsbad, CA, USA) and cDNA was synthesized from 100 ng of total RNA using TaqMan® Reverse Transcription Reagents (Applied Biosystems, Foster City, CA, USA). Reverse transcription was performed at 25°C for 10 min, 48°C for 30 min, and then 95°C for 5 min. cDNA was analyzed by qPCR using TaqMan® Universal PCR Master Mix (Applied Biosystems) in an Applied Biosystems StepOne™/StepOnePlus™ Real-Time PCR System. Cycling conditions for PCR amplification were 50°C for 2 min and 95°C for 10 min, followed by 40 cycles of 95°C for 10 s, then 60°C for 1 min. Relative quantification was achieved by normalizing to the β-actin gene (Applied Biosystems). The following probes were purchased from Applied Biosystems: *Ifng* (99999071_m1), *Tnf* (99999068_m1) and *Actb* (01205647_g1).

In vitro Proliferation Assays

APCs, PDCA-1^{+} pDCs from the livers of C57BL/6 mice, CD11b^{+} Mφs from the inflamed livers of Con A-injected C57BL/6 mice (Con A Mφs), IL-10$^{-/-}$ mouse Mφs, and DSS-treated C57BL/6 mouse Mφs (DSS Mφs) were isolated using a FACS Aria (Becton Dickinson Co.). Enriched naïve CD4^{+} splenocytes obtained from OT-II mice were sorted using a CD4^{+} CD62L^{+} T Cell Isolation Kit II (Miltenyi Biotech, Auburn, CA, USA) and labeled with 1 mM CFSE (Molecular Probes, Eugene, OR, USA) for 10 min at 37°C, followed by the addition of 1.0 ml of FCS for 2 min and washed three times in PBS. CFSE-labeled CD4+ naïve cells (1×10^5 cells/well) were co-cultured with pDCs or Mφs (2×10^4 cells/well) in 96-well round-bottom plates for 72 h in the presence of OVA peptides (1 μM). After incubation, cells were collected, incubated with anti-CD4-PE-Cy7 and anti-CD3e-APC-Cy7 and analyzed by FACS; 7-AAD was added to exclude dead cells. Proliferation analysis is based on division times of CFSE^{+}CD4^{+} T cells.

Unlabeled CD4^{+} naïve T cells (1×10^5 cells/well) were also co-cultured with pDCs or Mφs (2×10^4 cells/well) for 120 h in the presence of OVA peptides followed by incubation with anti-IFN-γ and/or anti-IL-17 mAbs, and then treated with a Cytofix/Cytoperm kit (BD bioscience). Culture supernatant was collected and analyzed with the BD™ Cytometric Beads Array Mouse Th1/Th2/Th17 Cytokine Kit (Becton Dickinson Co.).

Statistical Analysis

Results are expressed as mean ± SEM. Data groups were analyzed with GraphPad Prism using Tukey-Kramer test and Student's *t*-tests. A *P*-value less than 0.05 was considered statistically significant.

Results

Accumulation of Mononuclear Cells was Induced in the Liver of Mice with Chronic Colitis

To investigate hepatic immunological regulation in the colitic condition, we first used two murine IBD models, RAG-2$^{-/-}$ mice adoptively transferred with splenic CD4^{+}CD45RB^{high} T cells from WT mice (RAG-2$^{-/-}$ RB^{high} mice) and IL-10$^{-/-}$ mice. Consistent with previous reports [15], RAG-2$^{-/-}$ RB^{high} mice showed severe colitis, and infiltration of mononuclear cells in the portal vein area of the liver (Fig. 1A). This was not observed in WT mice. IL-10$^{-/-}$ mice spontaneously developed colitis, characterized by prominent epithelial hyperplasia with leukocyte infiltration into the liver (Fig. 1A). Consistently, the absolute number of liver

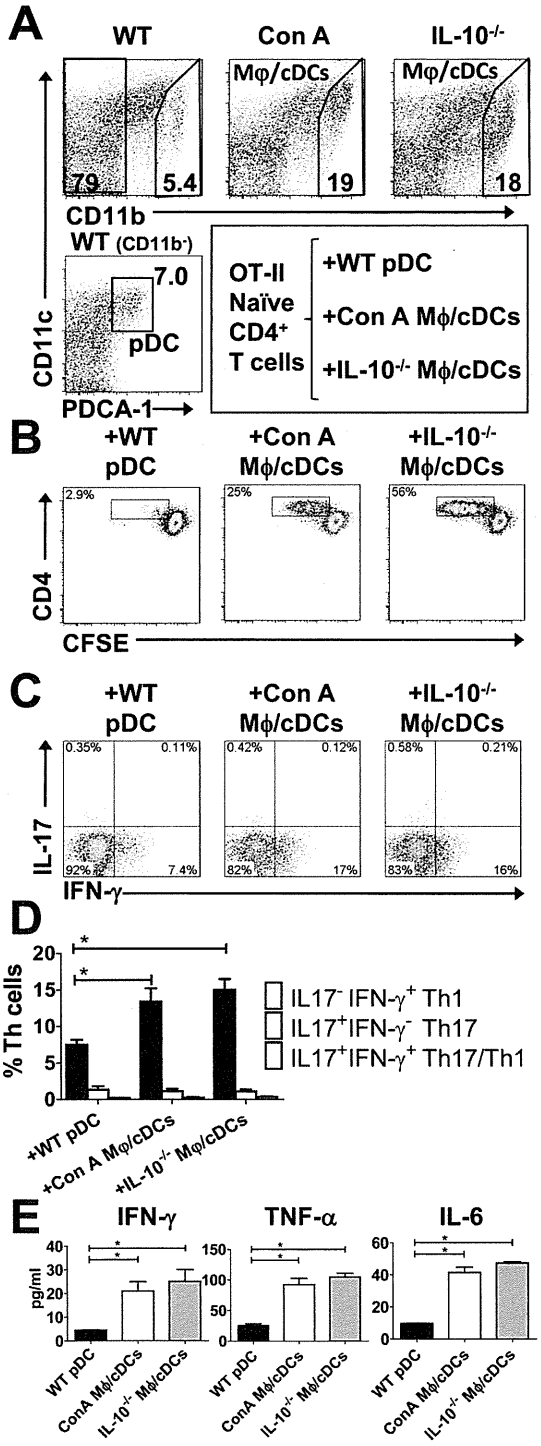

Figure 3. Hepatic Mφ/cDCs cells under colitic conditions induce a Th1 inflammatory response. (**A**) FACS analysis of PDCA-1$^+$CD11b$^-$CD11c^{int} pDCs from the livers of WT (left column) mice. We also analyzed CD11b$^+$CD11c$^-$ Mφs from the livers of ConA-treated (middle) and IL-10$^{-/-}$ (right) mice, respectively. Dead cells were excluded with 7AAD staining. (**B**) Proliferation of naïve CFSE-labeled splenic CD4$^+$ T cells from OT-II mice, and co-cultured WT pDCs, ConA Mφs, or IL-10$^{-/-}$ Mφs in the presence of OVA. Dead cells were excluded with 7AAD staining and CD4$^+$ T cells gated on CD3$^+$ CD4$^+$ cells are shown (B and C). Data are representative of three independent experiments. (**C**) Intracellular IFN-γ and IL-17A expression in CD4$^+$ T cells co-cultured with WT pDCs, ConA Mφs, or IL-10$^{-/-}$ Mφs in the presence of OVA. Data are representative of three independent experiments. (**D**) Proportion of IFN-γ$^+$IL-17A$^-$, IFN-γ$^-$IL-17A$^+$, and IFN-γ$^+$IL-17A$^+$ cells among the Th cell population. (**E**) Cytokine concentrations in the culture supernatant of OT-II CD4$^+$ T cells that were co-cultured with WT pDCs or ConA Mφs. Data are representative of three independent experiments. Each experiment was performed using duplicate samples. *P<0.05.

doi:10.1371/journal.pone.0084619.g003

mononuclear cells in both colitis models was significantly increased when compared with age-matched C57BL/6 mice (Fig. 1B). Liver enzymes (aspartate aminotransferase and alanine aminotransferase) demonstrated no significant changes between WT mice and the two colitis groups (data not shown).

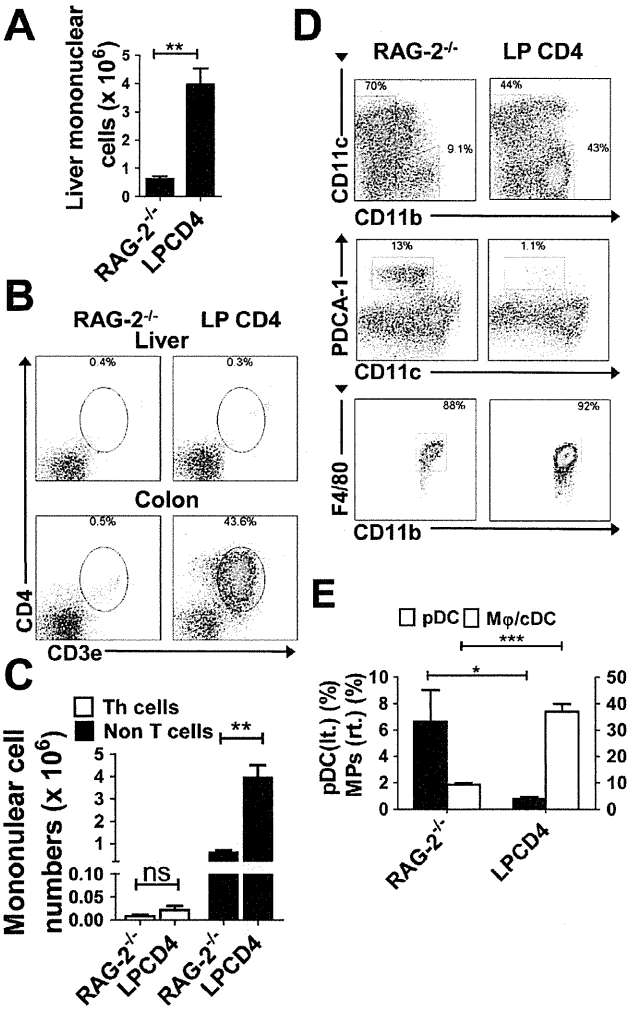

Figure 4. Immune dysregulation in the liver independent of T cell accumulation in the liver. (**A**) Numbers of hepatic mononuclear cells. Data are presented as the mean ± SEM for each group. RAG-2$^{-/-}$ mice (n=4) and RAG-2$^{-/-}$ LP CD4$^+$ mice (n=4). (**B**) Representative data from flow cytometry analysis of Th cells in each organ. Dead cells were excluded by 7AAD staining. (**C**) Numbers of hepatic CD3$^+$ CD4$^+$ Th cells and non-T cells. (**D**) Representative data from flow cytometry analysis of pDCs and Mφs in the liver of each experimental group. Dead cells were excluded using 7AAD staining. Scatter plots for CD11b$^-$CD11c^{int} and CD11b$^+$CD11c$^-$ cells are shown in the middle and bottom rows, respectively. (**E**) Proportion of PDCA-1$^+$CD11b$^-$CD11c^{int} pDCs and F4/80$^+$CD11b$^+$CD11c$^-$ Mφs among whole mononuclear cells. Data are representative of three independent experiments. Values are presented as the mean ± SEM from seven mice in each group. *P<0.05, **P<0.01, ***P<0.005.

doi:10.1371/journal.pone.0084619.g004

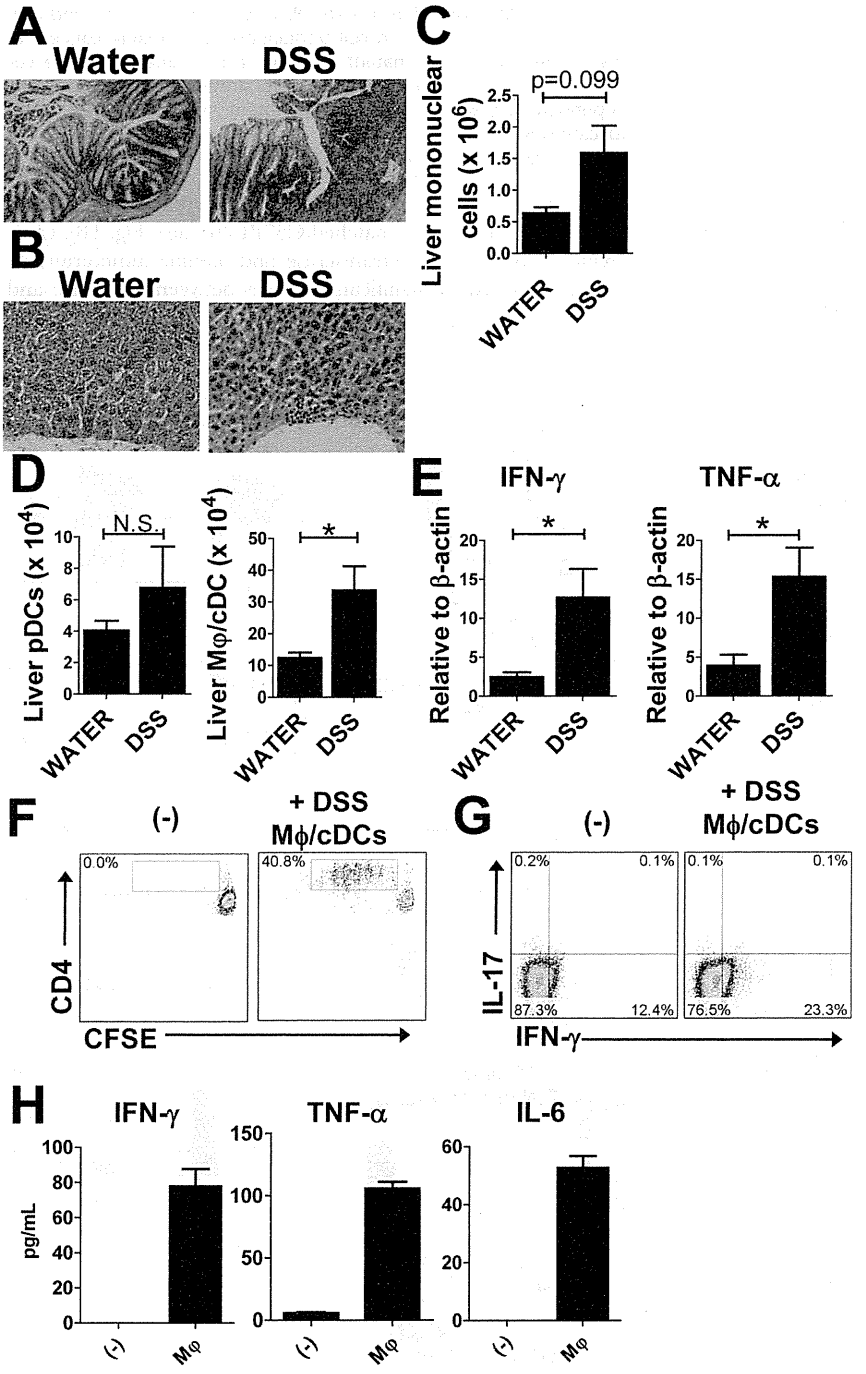

Figure 5. Accumulation of liver macrophages in acute colitis models. (**A**) H&E specimens of the colon taken from mice treated with water (left) or 2% DSS (right). Magnification, ×40 (**B**) H&E specimens of livers from mice treated with water (left) and DSS (right). Magnification, ×100 (**C**) The number of liver mononuclear cells from water- and DSS-treated mice. (**D**) The absolute number of PDCA-1^{+}CD11b^{-}CD11c^{int} pDCs and CD11b^{+}CD11c^{-} Mφs among whole mononuclear cells. Data are representative of three independent experiments. (**E**) Levels of mRNA transcripts for IFN-γ, TNF, and IL-6 in the liver. Values are presented as the mean ± SEM for each group ($n=4$, water-treated group; $n=5$, DSS-treated group). *$P<0.05$. N.S., no significant difference. (**F–H**) Hepatic DSS Mφs induce a Th1 inflammatory response. (**F**) Proliferation of naïve CFSE-labeled splenic CD4^{+} T cells. (**G**) Intracellular IFN-γ and IL-17A expression in naïve CFSE-unlabeled splenic CD4^{+} T cells from OT-II mice that were co-cultured with or without hepatic Mφs from DSS-treated WT mice in the presence of OVA. Dead cells were excluded with 7AAD staining, and CD4^{+} T cells gated on CD3^{+} CD4^{+} cells are shown. Data are representative of two independent experiments. (**H**) Representative cytokine concentrations in culture supernatants from two independent experiments. Each experiment was performed using duplicate samples.
doi:10.1371/journal.pone.0084619.g005

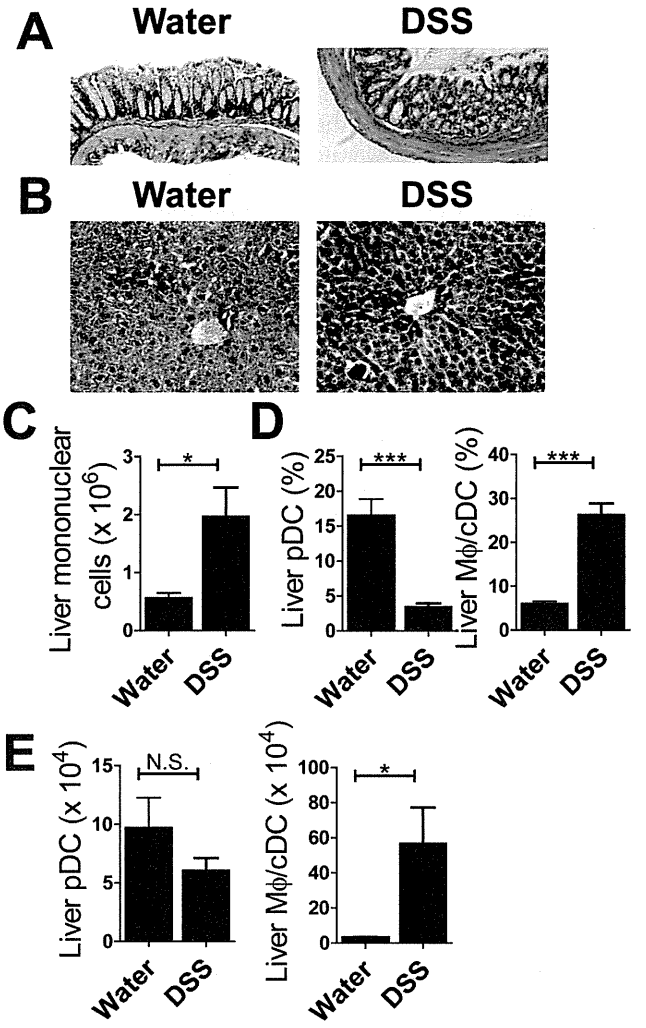

Figure 6. Hepatic infiltration of Macrophages are obserbed in DSS-treated RAG-2$^{-/-}$ mice. (**A**) H&E specimens of colon from mice treated with water (left) or 4% DSS (right). Magnification, ×100 (**B**) H&E specimens of liver from water- (left) and DSS-treated (right) mice. Magnification, ×200 (**C**) The number of liver mononuclear cells for each group of mice. (**D**) Proportion and (**E**) absolute number of PDCA-1^{+}CD11b^{-}CD11c^{int} pDCs and CD11b^{+}CD11c^{-} macrophages among whole mononuclear cells. Data are representative of two independent experiments. Values are presented as the mean ± SEM for each group ($n=4$, water-treated group; $n=4$, DSS-treated group). *$P<0.05$. N.S., no significant difference.
doi:10.1371/journal.pone.0084619.g006

Chronic Colitis is Associated with APC Balance in the Liver

Since it has been reported that Mφ/cDCs and pDCs represent subgroups of APCs differentiated from Mφ/DC precursors [23], we further investigated the composition of APCs in the liver. Analysis of flow cytometry data revealed that the proportion of CD11b^{+}CD11c$^{high/low}$ Mφ/cDCs in the livers (Fig. 2A, first row) of RAG-2$^{-/-}$ RB^{high} and IL-10$^{-/-}$ mice was significantly increased when compared with WT mice. Almost all CD11b^{+}CD11c$^{high/low}$ Mφ/cDCs expressed F4/80 (Fig. 2A, third and fourth rows), therefore we classified them as mononuclear phagocyte system cells. In contrast, the proportion of CD11b^{-}CD11c^{low}PDCA-1^{+} pDCs in the livers of WT mice was significantly higher than those in RAG-2$^{-/-}$ RB^{high} and IL-10$^{-/-}$ mice (Fig. 2A, second row). Statistical analysis confirmed reciprocal changes, where a decrease in the proportion (and absolute number) of pDCs corresponded to an increase in Mφ/cDCs in the liver of colitic mice (Fig. 2B). F4/80^{+}CD11b^{+}CD11c^{high} cells, but not F4/80^{+}CD11b^{+}CD11c^{low} cells, were predominant in hepatic Mφ/cDCs (Fig. 2C). Only a small number of pDCs were found in the LP of the colon under both healthy and colitic conditions (Fig. 2D and E).

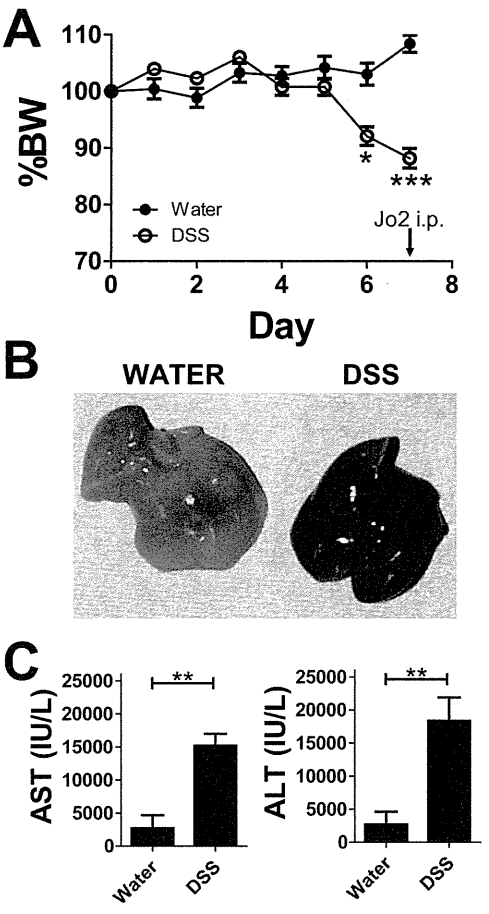

Figure 7. Newly recruited macrophages in the liver during colitis predispose it to inflammation. WT mice were treated under SPF conditions with 2% DSS for 5 days and subsequently with water for 2 days ($n=5$ mice per group). The Fas-activating antibody, Jo2, was injected i.p. into mice. (**A**) Changes in body weight are expressed as a percentage of original weight. Values are presented as the mean ± SEM for each group. Data are representative of two independent experiments. (**B**) Macroscopic view of livers from water- (left) and DSS-treated mice. (**C**) Levels of aspartate aminotransferase (left) and alanine aminotransferase (right) in water- and DSS-treated mice 6 h after Jo2 injection.
doi:10.1371/journal.pone.0084619.g007

Hepatic Mφ/cDCs Under Colitic Conditions Induce a Th1 Inflammatory Response

Owing to finding drastic compositional changes of liver APCs in colitic conditions, we assessed the function of hepatic CD11b^{-}CD11c^{low}PDCA-1^{+} pDCs isolated from the livers of WT mice (WT pDCs), and CD11b^{+}CD11c$^{-/+}$ Mφ/cDCs isolated from the livers of colitic IL-10$^{-/-}$ mice (IL-10$^{-/-}$ Mφ/cDCs) (Fig. 3A). The positive controls were Mφ/cDCs isolated from ConA-treated livers (ConA Mφ/cDCs) (Fig. 3A). We co-cultured pDCs or Mφ/cDCs with naïve CFSE-labeled CD4^{+} T cells in the

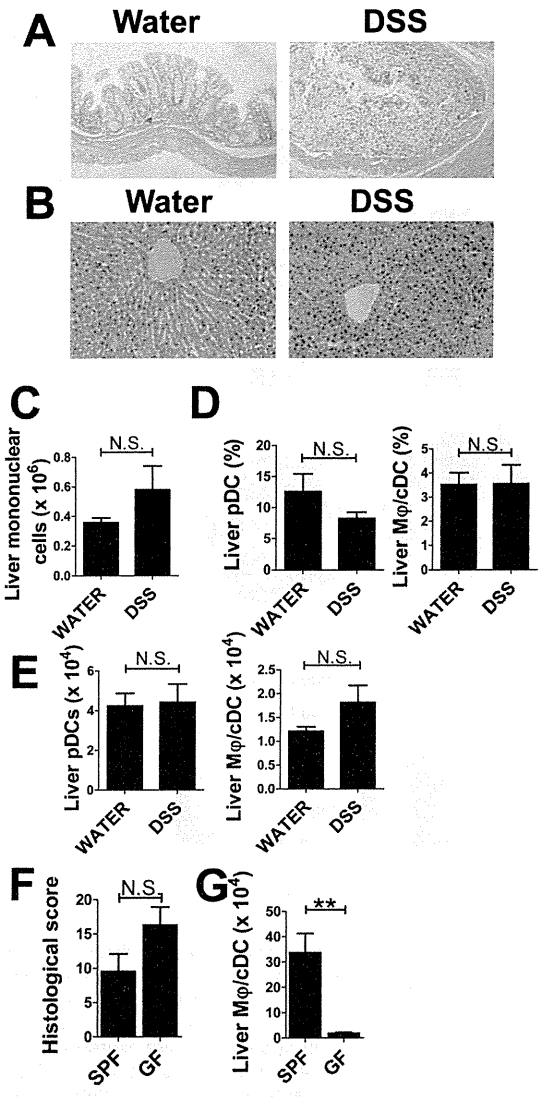

Figure 8. GF condition abrogates the compositional changes of hepatic APCs in acute colitis models. (**A**) H&E staining of colon sections taken from mice treated with water (left) or DSS (right). Magnification, ×100. (**B**) H&E staining of liver sections from water- (left) and DSS-treated (right) mice. Magnification, ×100. (**C**) Number of liver mononuclear cells. (**D**) Proportion and (**E**) absolute number of PDCA-1$^+$CD11b$^-$CD11c^{int} pDCs and CD11b$^+$CD11c$^-$ Mφs among whole mononuclear cells. (**F, G**) Comparisons between SPF and GF in the histology (F) and the numbers of Mφs (G) in DSS-treated mice. Data are representative of two independent experiments. Values are presented as the mean ± SEM for each group ($n = 5$, water-treated GF group; $n = 4$, DSS-treated GF group; $n = 5$, DSS-treated SPF group). N.S., no significant difference.

doi:10.1371/journal.pone.0084619.g008

presence of OVA peptides. After 72 h in culture, CD4$^+$ T cells had extensively divided in the presence of Mφ/cDCs from not only Con A-treated mice but also colitic IL-10$^{-/-}$ mice, but divided little in the presence of WT pDCs (Fig. 3B). To further assess pro-inflammatory responses of Mφ/cDCs, we examined cytokine production from cultured CD4$^+$ T cells. Flow cytometry showed a significant increase in the proportion of IFN-γ-expressing CD4$^+$ T cells following co-culture with IL-10$^{-/-}$ Mφ/cDCs. A similar result was seen with ConA Mφ/cDCs; however, there was no significant increase in IL-17-producing CD4$^+$ T cells (Fig. 3C and D). Consistent with these data, culture supernatants from CD4$^+$ T cells following co-culture with IL-10$^{-/-}$ Mφ/cDCs or ConA Mφ/cDCs exhibited a significant increase in IFN-γ and other pro-inflammatory cytokines such as IL-6 and TNF-α (Fig. 3E).

Immune Dysregulation in the Liver

Given the evidence that activated Mφ/cDCs in the liver instruct naïve CD4$^+$ T cells to differentiate into Th1 cells (Fig. 3C), we then examined whether the primary recruitment of colitogenic Th1 cells to the liver or other mechanisms induced a dysregulation in the balance of Mφ/cDCs and pDCs in the liver under colitic conditions, as mononuclear cells expanded in the liver in colitic RAG-2$^{-/-}$ RB^{high} mice and IL-10$^{-/-}$ mice (Fig. 1). As an alternative mechanism, the breakdown of the colonic barrier and sequential uptake of MAMPs or other gut-derived antigens during the colitis state may play an important role in drastic changes of APCs in the liver. To minimize the effects of liver-infiltrating T cells, we used an adoptive retransfer system: colitogenic LP CD4$^+$ T cells obtained from established RAG-2$^{-/-}$ RB^{high} mice were transferred into RAG-2$^{-/-}$ mice to generate RAG-2$^{-/-}$ LP CD4$^+$ mice, as colitogenic CD4$^+$ T cells residing in the intestine express gut-specific homing receptors and have an ability to preferentially migrate to the intestine but not to liver [24,25]. These mice developed severe colitis (data not shown) and also showed significant increases in the number of liver-infiltrating mononuclear cells (Fig. 4A). The RAG-2$^{-/-}$ LP CD4$^+$ mice showed almost no CD3$^+$CD4$^+$ T cell infiltration in the liver, but did exhibit severe colitis with marked infiltrations of CD3$^+$CD4$^+$ T cells in the colon (Fig. 4B). We confirmed statistically that the significant increases in liver mononuclear cells in RAG-2$^{-/-}$ LP CD4$^+$ mice was due to the emergence of non-T cells (possibly APCs) (Fig. 4C). We further investigated compartments of APCs in the liver of RAG-2$^{-/-}$ LP CD4$^+$ mice. Consistent with the data from colitic RAG-2$^{-/-}$ RB^{high} or IL-10$^{-/-}$ mice (Fig. 2), RAG-2$^{-/-}$ LP CD4$^+$ mice also showed reciprocal changes; a significant decrease in pDCs corresponded with an increase in Mφ/cDCs (Fig. 4D and E). RAG-2$^{-/-}$ LP CD4$^+$ mice exhibited severe colitis without infiltration of T cells in the liver (Fig. 4B and 4C). These data suggest that intestinal inflammation induce changes in the compartments of APCs.

Accumulation of Mφ/cDCs in the Livers of Mice with DSS-induced Colitis

To further determine whether hepatic immune dysregulation is caused by barrier disruption of the intestinal wall, we looked at livers from immune-sufficient WT mice subjected to DSS-induced colitis under SPF conditions. Seven days after the start of DSS administration, mice exhibited severe colitis and infiltration of mononuclear cells in the liver (Fig. 5A and B). Consistent with histological data, liver mononuclear cells were upregulated in DSS-treated mice when compared with water-treated mice (Fig. 5C). Flow cytometry revealed that the number of Mφ/cDCs was significantly increased in the livers of DSS-treated mice; however, there were no significant changes in the numbers of pDCs (Fig. 5D). Expression levels of IFN-γ and TNF-α in the liver were significantly increased in DSS-treated mice (Fig. 5E). Furthermore, hepatic Mφ/cDCs in the DSS-treated mice promoted proliferation of CD4$^+$ T cells (Fig. 5F), and increased the proportion of IFN-γ-expressing CD4$^+$ T cells (Fig. 5G). We detected a significant increase in pro-inflammtory cytokines in co-culture supernatants (Fig. 5H).

We also confirmed the reciprocal changes for pDCs and Mφ/cDCs in DSS-treated RAG-2$^{-/-}$ mice, which had severe colitis and infiltration of mononuclear cells in the liver (Fig. 6A, B and C). The proportion of pDCs was decreased in DSS-treated RAG-2$^{-/}$

$^{-}$ mice (Fig. 6D). Furthermore, the proportion and number of Mφ/cDCs was increased, even in mice lacking $CD4^+$ T cells (Fig. 6D and E). These data suggest that colon inflammation induces the recruitment of Mφ/cDCs and these newly recruited Mφ/cDCs stimulate Th1 cells or promote differentiation of Th1 cells.

We also assessed whether these Mφ/cDCs that emerged under colitic conditions contributed to acute liver inflammation, which had been initially induced by Fas-activating antibody (Jo2) [18,19]. As shown in Fig. 7A, DSS-treated mice with significant body weight loss underwent Jo2 treatment. The livers of DSS-induced colitic mice in which Jo2 was administered showed significant blood accumulation (Fig. 7B). Consistently, the levels of aspartate aminotransferase and alanine aminotransferase were significantly increased in DSS mice after Jo2 treatment compared with non-DSS mice (Fig. 7C).

Leukocyte Infiltration was not Detected in Acute Colitis Models Under GF Conditions

We investigated whether MAMPs or other bacterial degradation products induce hepatic immune dysregulation and analyzed the livers of mice treated with DSS under GF conditions. Bacteria do not reside in the intestines of GF mice, meaning there is no inflow of bacterial components into the liver. Mice treated with DSS under GF conditions showed severe colitis; however, there was no evidence of leukocyte infiltration (Fig. 8A and B). Consistent with histological data, we observed no significant changes in the number of liver mononuclear cells for controls and DSS-treated mice (Fig. 8C). Flow cytometry data showed that there were no significant changes in the ratios of pDCs to Mφ/cDCs (Fig. 8D); or in the absolute numbers of these cells in the livers of DSS-treated mice (Fig. 8E). DSS-treated GF mice also exhibited severe colitis compared with SPF mice (Fig. 8F), but Mφ/cDCs were not increased (Fig. 8G). These findings indicate that bacterial products play a crucial role in inducing infiltration of Mφ/cDCs into the liver.

Discussion

In this study we demonstrated: (1) hepatic pDCs are decreased and Mφ/cDCs are increased in mice with chronic intestinal inflammation; (2) newly emerged Mφ/cDCs during the development of colitis possess pro-inflammatory characteristics that drive differentiation of naïve T cells toward Th1 cells; (3) Mφ/cDCs that emerge during colitis possibly result in the exacerbation of hepatitis symptoms; and (4) the reciprocal changes we observed in the compartments of the liver's innate immune system during intestinal inflammation were mainly caused by MAMPs, other bacterial degradation products, or bacteria themselves subsequent to the disruption of the intestinal wall. Changes in APC compartments were seen not only in RAG-$2^{-/-}$ RB^{high} mice and DSS-administered mice but also in RAG-$2^{-/-}$ mice retransferred with gut-tropic colitogenic LP $CD4^+$ T cells in SPF conditions; but were not seen in mice of the DSS colitis model in the GF condition that lack commensal bacteria in the gut.

Previous studies have suggested a relationship between intestinal and liver inflammation [2,3,11,26]. These previous reports support our hypothesis that intestinal inflammation skews the balance of immune cells in the liver. However, no expansive research has been conducted to clarify the inflammatory relationship between the liver and the intestine. In this study, we are the first to demonstrate distinctive changes in compartments (pDCs vs. Mφ/cDCs) of hepatic immune cells due to chronic intestinal inflammation. Increased hepatic Mφ/cDCs appeared irrespective of whether the colitis model was acute or chronic. Immunological changes were not only observed in the liver during colitis, but also in ConA-induced liver injury (Fig. 3A) [14], suggesting that these changes are universal phenomena during liver stress.

We hoped to elucidate how these crucial changes of hepatic APCs occur during intestinal inflammation. The liver is between the portal and systemic circulatory systems. The liver receives continuous blood supplements from the intestine via the portal vein and is presumably exposed to MAMPs or other degradation products from viable or non-viable commensal bacteria [8]. We used a GF system to demonstrate the importance of bacterial components in causing immunological dysregulation in the liver. Most models of experimental colitis fail to develop under GF conditions [27,28]; however, we used a DSS model, which is known to result in the development of severe colitis [29,30]. DSS-treated mice under SPF conditions exhibited Mφ/cDC infiltration into the liver (Fig. 5 and 8). This was not observed for DSS-treated mice under GF conditions despite the existence of severe colitis. This means that the accumulation of Mφ/cDCs is not just a consequence of nonspecific inflammation related with colitis. Mice under GF conditions lack the protective effects against colitis from microbiota [31], but also lack the stimulant transferred from the intestine to the liver. These data suggest that stimulation from degradation products from intestinal commensal bacteria play an important role in recruitment of Mφ/cDCs.

Various commensal bacteria that usually reside in the intestine (such as *C. coccoides*, *C. leptum* and *Enterococcus)* were found in ConA-treated and untreated livers [20]. Such a finding lends support to the hypothesis that intestinal bacterial products or bacteria themselves are transferred from the intestine to the liver. The rate (and amount) of uptake of bacteria-derived products, such as microbial DNA and LPS, is thought to increase during colitis because of the fragility of the colon wall [11,32]. Further study is required to estimate the amount and type of bacterial products that stimulate the liver during colitis.

Despite our finding that recruitment of Mφ/cDCs is stimulated by bacterial degradation products or bacteria themselves, several scenarios may be considered as additional mechanisms underlying the accumulation of Mφ/cDCs. First, activated Mφ/cDCs themselves migrate from the intestine to the liver. Alternatively, circulating monocytes accumulate in the liver stimulated by pro-inflammatory cytokines transferred via the portal vein, such as TNF-α produced by LP $CD4^+$ T cells or APCs in the intestine [30]. However, pro-inflammatory cytokines are produced in the colon of GF mice, so this possibility may only have a partial effect. Whether increased Mφ/cDCs originate from monocytes or resident macrophages in the liver should be explored in future studies. Third, activated T cells migrate from the intestine to the liver and stimulate the liver to recruit and activate circulating or resident Mφ/cDCs. RAG-$2^{-/-}$ LP $CD4^+$ mice (Fig. 3) and DSS-treated RAG-$2^{-/-}$ (Fig. 6) mice show increased Mφ/cDCs without infiltration of T, B, and NKT cells in the liver, which suggests that Mφ/cDCs are recruited to the liver independently of T, B, and NKT cells. However, there still remains involvement of cytokines, DSS itself and other types of the cells such as NK cells and liver sinusoidal endothelial. Macrophages accumulated during both acute and chronic colitis models in the liver produced inflammatory cytokines and promoted differentiation of Th1 cells or activation of NK cells. Thus, it is likely that systemic IFN-γ production leads subsequent upregulation of the sensitivity of FAS-mediated signal in the liver.

The current study suggests that hepatic APC compartments alter in parallel with the progression of colitis, and increased Mφ/

cDCs have pro-inflammatory characteristics. Two major hepatic diseases presenting as extraintestinal manifestations in IBD patients are PSC and autoimmune hepatitis. The prevalence of these liver diseases is reported, both in Crohn's disease and ulcerative colitis, to correlate with the severity and expansion of the intestinal disease [3,26,33]. The active disease is associated with ongoing extraintestinal manifestations in patients with Crohn's disease [26]. The prevalence of PSC was 5.5% in patients with substantial colitis and 0.5% in patients with distal colitis [2]. Therefore, Mφ/cDCs infiltrating into the liver in the colitis models may be involved in the pathogenesis of IBD-related liver diseases. However, liver enzymes demonstrated no significant changes during colitis unlike autoimmune hepatitis or PSC. Thus, we hypothesized that accumulated Mφ/cDCs may increase the susceptibility of hepatitis. We combined the Fas-mediated model of hepatitis with the DSS colitis models to show the clinical importance of our study. Fas-mediated hepatitis models are widely used as a model of hepatitis [18,19]. TNF-α released by activated hepatic macrophages is one of the very important factors that damage hepatocytes, which are highly sensitive to cell-extrinsic stimulation in Fas-mediated hepatitis [19]. We also suggest the importance of the infiltration of macrophages in fulminant hepatitis models [10]. Mφ/cDCs recruited to the liver during colitis in a T cell-independent manner produce pro-inflammatory cytokines and promote Th1 reaction. $CD11b^{+}CD11c^{low/+}$ Mφ/cDCs are already detectable in healthy WT mice (Fig. 2B), but previous studies suggest that these resident macrophages including Kupffer cells have a immunoregulatory character, such as producing IL-10 [6,34]. Taken together with the previous studies and our findings, Mφ/cDCs infiltrating into the liver during colitis may contribute to making the hepatitis worse. Some additional stimulation would be needed for breaking down liver tolerance and causing hepatitis or cholangitis which mimics liver diseases associated with IBD.

An additional finding of our study is that pDCs are significantly decreased in the late phase of colitis in the chronic models. Hepatic pDCs plays an important role in maintaining liver homeostasis [9,10,14], so not only increased Mφ/cDCs but decreased pDCs may have effects on the infiltration of mononuclear cells in the liver during chronic colitis. This is known as sustained negative regulation of LPS signaling in response to a second LPS stimulus. pDCs express certain toll-like receptors (TLR) [14], with the number of spleen pDCs decreasing following TLR treatment [35]. These previous reports suggest that pDCs are one of the initial sensors of MAMPs or other degradation products, and possibly decrease when the endotoxin tolerance is broken down. Further studies will be needed to address this issue.

In conclusion, the findings from our study suggest that dysregulation in the balance of liver APCs, especially in the recruitment of pro-inflammatory Mφ/cDCs, during colitis occurs in a T-cell-independent manner for chronic and acute murine colitis models. This report may provide the basis for a novel strategy to treat intractable immune diseases in the liver. We have also highlighted the relevance of the relationship between liver and intestine immunology during intestinal inflammation.

Acknowledgments

We thank A. Matsumoto, T. Handa, Y. Ono, N. Taniki, K. Takeshita, K. Saigusa and K. Kimura for their help with some of the experiments. We are grateful to M. K. Tokutake and M. Takabe for their assistance with the care of experimental animals.

Author Contributions

Conceived and designed the experiments: YM AY TK. Performed the experiments: YM SM NN AH. Analyzed the data: YM T. Sujino T. Sato KM T. Hisamatsu HE T. Hibi NK. Wrote the paper: YM AY TK.

References

1. Baumgart DC, Sandborn WJ (2007) Inflammatory bowel disease: clinical aspects and established and evolving therapies. Lancet 369: 1641–1657.
2. Olsson R, Danielsson A, Jarnerot G, Lindstrom E, Loof L, et al. (1991) Prevalence of primary sclerosing cholangitis in patients with ulcerative colitis. Gastroenterology 100: 1319–1323.
3. Rasmussen HH, Fallingborg JF, Mortensen PB, Vyberg M, Tage-Jensen U, et al. (1997) Hepatobiliary dysfunction and primary sclerosing cholangitis in patients with Crohn's disease. Scand J Gastroenterol 32: 604–610.
4. Tremaroli V, Backhed F (2012) Functional interactions between the gut microbiota and host metabolism. Nature 489: 242–249.
5. Kaisho T, Takeuchi O, Kawai T, Hoshino K, Akira S (2001) Endotoxin-induced maturation of MyD88-deficient dendritic cells. J Immunol 166: 5688–5694.
6. Crispe IN (2009) The liver as a lymphoid organ. Annu Rev Immunol 27: 147–163.
7. Crispe IN (2003) Hepatic T cells and liver tolerance. Nat Rev Immunol 3: 51–62.
8. Thomson AW, Knolle PA (2010) Antigen-presenting cell function in the tolerogenic liver environment. Nat Rev Immunol 10: 753–766.
9. Goubier A, Dubois B, Gheit H, Joubert G, Villard-Truc F, et al. (2008) Plasmacytoid dendritic cells mediate oral tolerance. Immunity 29: 464–475.
10. Tokita D, Sumpter TL, Raimondi G, Zahorchak AF, Wang Z, et al. (2008) Poor allostimulatory function of liver plasmacytoid DC is associated with pro-apoptotic activity, dependent on regulatory T cells. J Hepatol 49: 1008–1018.
11. Gabele E, Dostert K, Hofmann C, Wiest R, Scholmerich J, et al. (2011) DSS induced colitis increases portal LPS levels and enhances hepatic inflammation and fibrogenesis in experimental NASH. J Hepatol 55: 1391–1399.
12. Kamada N, Hisamatsu T, Okamoto S, Sato T, Matsuoka K, et al. (2005) Abnormally differentiated subsets of intestinal macrophage play a key role in Th1-dominant chronic colitis through excess production of IL-12 and IL-23 in response to bacteria. J Immunol 175: 6900–6908.
13. Kamada N, Hisamatsu T, Okamoto S, Chinen H, Kobayashi T, et al. (2008) Unique CD14 intestinal macrophages contribute to the pathogenesis of Crohn disease via IL-23/IFN-gamma axis. J Clin Invest 118: 2269–2280.
14. Nakamoto N, Ebinuma H, Kanai T, Chu PS, Ono Y, et al. (2012) CCR9(+) Macrophages Are Required for Acute Liver Inflammation in Mouse Models of Hepatitis. Gastroenterology 142: 366–376.
15. Powrie F, Leach MW, Mauze S, Caddle LB, Coffman RL (1993) Phenotypically distinct subsets of CD4+ T cells induce or protect from chronic intestinal inflammation in C. B-17 scid mice. Int Immunol 5: 1461–1471.
16. Ishii K, Kanai T, Totsuka T, Uraushihara K, Ishikura T, et al. (2004) Hyperexpression of inducible costimulator on lamina propria mononuclear cells in rat dextran sulfate sodium colitis. J Gastroenterol Hepatol 19: 174–181.
17. Kuhn R, Lohler J, Rennick D, Rajewsky K, Muller W (1993) Interleukin-10-deficient mice develop chronic enterocolitis. Cell 75: 263–274.
18. Murthy A, Defamie V, Smookler DS, Di Grappa MA, Horiuchi K, et al. (2010) Ectodomain shedding of EGFR ligands and TNFR1 dictates hepatocyte apoptosis during fulminant hepatitis in mice. J Clin Invest 120: 2731–2744.
19. Ogasawara J, Watanabe-Fukunaga R, Adachi M, Matsuzawa A, Kasugai T, et al. (1993) Lethal effect of the anti-Fas antibody in mice. Nature 364: 806–809.
20. Ojiro K, Ebinuma H, Nakamoto N, Wakabayashi K, Mikami Y, et al. (2010) MyD88-dependent pathway accelerates the liver damage of Concanavalin A-induced hepatitis. Biochem Biophys Res Commun 399: 744–749.
21. Mikami Y, Kanai T, Sujino T, Ono Y, Hayashi A, et al. (2010) Competition between colitogenic Th1 and Th17 cells contributes to the amelioration of colitis. Eur J Immunol 40: 2409–2422.
22. Kimura K, Kanai T, Hayashi A, Mikami Y, Sujino T, et al. (2012) Dysregulated balance of retinoid-related orphan receptor gammat-dependent innate lymphoid cells is involved in the pathogenesis of chronic DSS-induced colitis. Biochem Biophys Res Commun 427: 694–700.
23. Geissmann F, Manz MG, Jung S, Sieweke MH, Merad M, et al. (2010) Development of monocytes, macrophages, and dendritic cells. Science 327: 656–661.
24. Mora JR, Bono MR, Manjunath N, Weninger W, Cavanagh LL, et al. (2003) Selective imprinting of gut-homing T cells by Peyer's patch dendritic cells. Nature 424: 88–93.
25. Nemoto Y, Kanai T, Kameyama K, Shinohara T, Sakamoto N, et al. (2009) Long-lived colitogenic CD4+ memory T cells residing outside the intestine participate in the perpetuation of chronic colitis. J Immunol 183: 5059–5068.

26. Vavricka SR, Brun L, Ballabeni P, Pittet V, Prinz Vavricka BM, et al. (2011) Frequency and risk factors for extraintestinal manifestations in the Swiss inflammatory bowel disease cohort. Am J Gastroenterol 106: 110–119.
27. Podolsky DK (2002) Inflammatory bowel disease. N Engl J Med 347: 417–429.
28. Sartor RB (2006) Mechanisms of disease: pathogenesis of Crohn's disease and ulcerative colitis. Nat Clin Pract Gastroenterol Hepatol 3: 390–407.
29. Hayashi A, Sato T, Kamada N, Mikami Y, Matsuoka K, et al. (2013) A Single Strain of Clostridium butyricum Induces Intestinal IL-10-Producing Macrophages to Suppress Acute Experimental Colitis in Mice. Cell Host Microbe 13: 711–722.
30. Maslowski KM, Vieira AT, Ng A, Kranich J, Sierro F, et al. (2009) Regulation of inflammatory responses by gut microbiota and chemoattractant receptor GPR43. Nature 461: 1282–1286.
31. Rakoff-Nahoum S, Paglino J, Eslami-Varzaneh F, Edberg S, Medzhitov R (2004) Recognition of commensal microflora by toll-like receptors is required for intestinal homeostasis. Cell 118: 229–241.
32. Henao-Mejia J, Elinav E, Jin C, Hao L, Mehal WZ, et al. (2012) Inflammasome-mediated dysbiosis regulates progression of NAFLD and obesity. Nature 482: 179–185.
33. Bjornsson E, Olsson R, Bergquist A, Lindgren S, Braden B, et al. (2008) The natural history of small-duct primary sclerosing cholangitis. Gastroenterology 134: 975–980.
34. Knolle P, Schlaak J, Uhrig A, Kempf P, Meyer zum Buschenfelde KH, et al. (1995) Human Kupffer cells secrete IL-10 in response to lipopolysaccharide (LPS) challenge. J Hepatol 22: 226–229.
35. Swiecki M, Wang Y, Vermi W, Gilfillan S, Schreiber RD, et al. (2011) Type I interferon negatively controls plasmacytoid dendritic cell numbers in vivo. J Exp Med 208: 2367–2374.

Anson W. Lowe and Richard H. Moseley, Section Editors

Magnetic Resonance Imaging vs Enteroscopy in Crohn's Disease

Crohn's disease is an autoimmune process that may affect any segment of the gastrointestinal tract. In addition to the active disease that is often expressed as mucosal ulcerations, Crohn's disease can be a transmural process, affecting the entire wall of the intestine. In addition to the acute manifestations of the disease in the mucosa, chronic changes may result in stenosis or fistulas.

Early descriptions of Crohn's disease utilized radiography with barium contrast for diagnosis and monitoring. The major shortfall of barium studies, however, is their poor sensitivity for mucosal lesions. With the introduction of endoscopy, the ability to directly visualize and sample the affected mucosa greatly enhanced sensitivity for those areas that could be approached. Until recently, however, esophagogastroduodenoscopy and colonoscopy were limited to the extreme ends of the gastrointestinal tract.

Recent studies indicating that the presence or absence of mucosal lesions is a better indicator for a successful therapeutic response has stimulated a need for better approaches for detection, especially in regions of the small intestine that are not accessible by conventional endoscopy. Fortunately, several new diagnostic approaches have been developed that provide diagnostic options. From the endoscopic perspective, double- and single-balloon enteroscopy have enabled access to the entire gastrointestinal tract, and offers the advantage of direct visualization, the ability to obtain tissue, and a means of effecting therapy for lesions such as strictures. Recently enhanced approaches in imaging provide the means to noninvasively evaluate the small intestine, and provide the added benefit of visualizing extra-intestinal areas at the same time. These modalities include magnetic resonance imaging (MRI) enterography and compute tomographic enterography.

In this issue of *Gastroenterology*, Takenaka et al report on a prospective clinical trial comparing MRI enterography and balloon enteroscopy. A total of 100 Crohn's patients with mild to moderate disease were studied first with MRI enterography, which was followed within 3 days with either single (90 subjects) or double (10 subjects) balloon enteroscopy. The operators of each procedure, which consisted of 2 endoscopists and 2 radiologists, were blinded to the results of the other procedure. A retrograde approach was used for endoscopy, which successfully evaluated the entire intestine for 11%, the jejunum in 40%, and the proximal ileum in 98% of patients. Twenty patients were treated for stenotic lesions with balloon dilation. MRI enterography was able to detect active lesions in 11 patients that were beyond the reach of the endoscope. Mucosal abnormalities were classified as ulcerated lesions and all mucosal lesions by endoscopy, for which MRI enterography exhibited sensitivities in the small intestine of 82.4% (95% CI, 75.4%–87.7%) and 67.5% (95% CI, 63.1%–70.0%), respectively, with specificities of 87.6% (95% CI, 83.7%–90.6%) and 94.8% (95% CI; 90.1%–97.5%; Figure 1). MRI enterography, however, was less effective in detecting major stenosis with a sensitivity and specificity of 58.8% (95% CI, 37.6%–77.2%) and 90.0% (95% CI, 88.4%–91.5%), respectively.

See page 334.

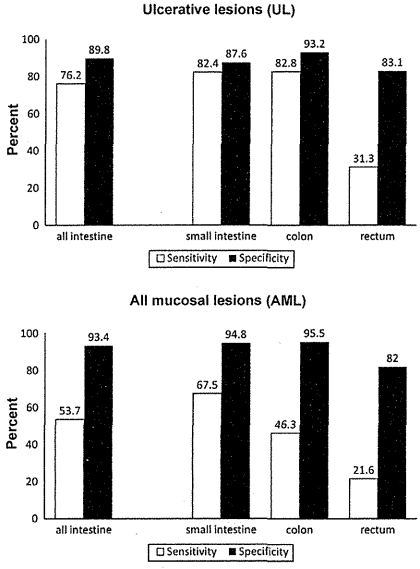

Figure 1. Sensitivity and specificity of magnetic resonance imaging (MRI) enterography for the detection of active lesions.

An Effective Interferon-Free Regimen for Hepatitis C Therapy

Developments are occurring in the approach to the treatment of patients chronically infected with the hepatitis C virus (HCV) at such a rapid pace that may make it difficult to keep up to date. One particular aspect—the requirement for ribavirin, which is associated with hemolytic anemia, rash, and teratogenicity, in these new treatment regimens, which include agents such as sofosbuvir (a nucleotide NS5B inhibitor), ledipasvir (an NS5A inhibitor), daclatasvir (an NS5A inhibitor), and asunaprevir (an NS3/4A inhibitor)—has been the focus of recent studies. In this issue of *Gastroenterology*, Andreone et al report the results of a multicenter, open-label phase 3 trial of a 12-week, all-oral, interferon-free regimen of the NS3/4A protease inhibitor, ABT-450/r (co-dosed with the CYP3A4 inhibitor, ritonavir, to allow for once-daily dosing), co-formulated with the NS5A inhibitor, ombitasvir (previously ABT-267), and the non-nucleoside polymerase inhibitor, dasabuvir (formerly ABT-333) twice daily, with (group 1) or without ribavirin (group 2), in 179 noncirrhotic, pegylated interferon/ribavirin treatment-experienced patients chronically infected with HCV genotype (GT) 1b, the most prevalent subgenotype worldwide.

Sustained virologic response was achieved after 12 weeks (SVR12) of treatment in 96.6% and 100% of group 1 and 2 patients, respectively (Figure 2). Of the group 1 patients who did not achieve SVR12, 2 patients discontinued treatment owing to adverse events not thought to be study drug-related. SVR in both groups was not influenced by

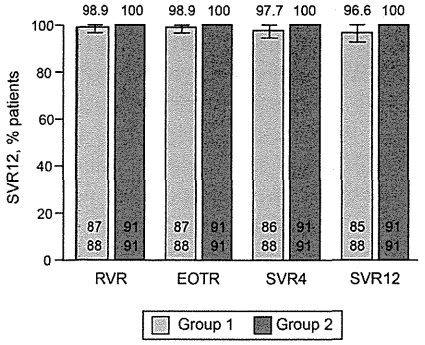

Figure 2. ITT genotype 1b efficacy subset treatment response over time. Percentage of patients achieving virologic response (±95% CIs) are presented for week 4 of treatment (RVR), end of treatment (EOTR), 4 weeks post-treatment (SVR4), and SVR12, as well as n/N within the bars graphs.

previous nonresponse, age, race, or interleukin-28B genotype. Fatigue, headache, and nausea were the most common reported adverse events in both groups; as expected, group 1 patients had more events associated with ribavirin use, including fatigue, nausea, insomnia, anemia, rash, and elevated serum bilirubin. These findings confirm previous results and support consideration of the use of this multitargeted treatment regimen, without the addition of ribavirin, in the treatment of HCV GT1b-infected, treatment-experienced patients without cirrhosis. In contrast, ribavirin may offer benefit in HCV GT1a-infected patients.

See page 359.

Unique DNA Methylation Profiles in Colonic Adenomas

DNA methylation is a form of epigenetics that functions in the regulation of gene expression. It involves the addition of a methyl group to cytosine to form 5-methylcytosine, which can result in the repression of gene expression. DNA methylation most often occurs at CpG dinucleotides. CpGs are underrepresented in the genome and occur at a frequency lower than what would be expected from random chance. CpG islands are regions of the genome of ≥200 bp that contain CpGs at high frequency, which is most often observed in the region of promoters.

With respect to cancer, DNA methylation that represses the expression of a tumor suppressor may be important in pathogenesis. In general, cancer tissues exhibit greater levels of DNA methylation. In this issue of *Gastroenterology*, Luo et al report on their profiling of DNA methylation in colonic adenomas, cancer, and normal tissues. To perform these studies, the authors performed a genome-wide characterization using microarray technology that enables an assessment of >485,000 methylation sites. The technology was used to assess the methylation status of tissues derived from 41 normal colons, 42 colonic adenomas, and 64 colon cancers.

The authors found progressively greater epigenetic alterations as one progressed from normal colons to adenomas, and finally cancer. Even when colonic tissue from normal individuals was compared with tissue derived from normal colonic tissue adjacent to colorectal cancer, there was already evidence of greater methylation levels in the latter group. The authors concluded that changes in DNA methylation status occur very early in colon cancer pathogenesis. As the analysis progressed from adenomas to cancer, there was also evidence of increasing epigenetic alterations with both hypo- and hypermethylation detected compared with normal colons. There was also an increase in the variability of epigenetic changes with progression to cancer (Figure 3).

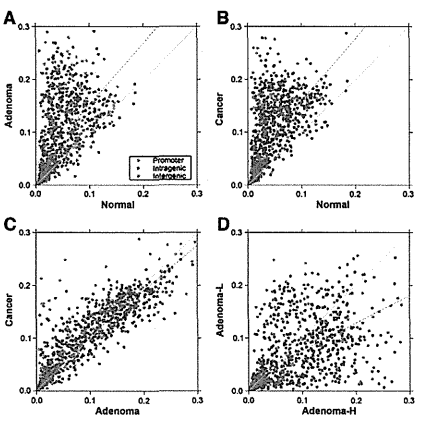

Figure 3. Intersample variability of 1000 randomly selected probes for the samples designated for each axis. Each point represents the standard deviation.

The authors used clustering algorithms to stratify adenomas into different groups based on their methylation profiles. The authors proposed that the methylation differences observed between groups suggested an origin from different stem cell precursors. The clustering analysis also suggested that the stratification of adenomas based on DNA methylation patterns may provide insights into the likelihood into developing colorectal cancer.

See page 418.

First Genome-Wide Association Study of Autoimmune Hepatitis Type I

Autoimmune hepatitis (AIH) is characterized by the presence of serum autoantibodies (antinuclear, smooth muscle, and soluble liver antigen/liver pancreas antibodies in type I AIH and liver kidney microsomal-1 antibodies in type II AIH), elevated serum immunoglobulin G levels, and interface hepatitis on histologic examination. However, the genetic risk factors for this low-prevalence autoimmune liver disease are unknown other than the reported association in small study populations of certain HLA class-II genotypes (DR3 and DR4) with AIH. Increasingly, genome-wide association studies have been used to identify genetic susceptibility loci in disease states, including liver diseases such as primary biliary cirrhosis (PBC) and primary sclerosing cholangitis (PSC).

In this issue of *Gastroenterology* (accompanied by an editorial), de Boer et al have applied this methodology in a discovery cohort of 649 Dutch adult patients with type I AIH and 13,436 control subjects and compared their findings in a replication cohort of 451 German adult patients and 4,103 control subjects. In both cohorts, the most prominent association was found at *rs2187668*, which maps to the intronic region of the *HLA-DQA1* gene on chromosome 6 and is an efficient tagging single nucleotide polymorphism for the *HLA-DRB1*0301* and *HLA-DRB1*0401* haplotypes. The strongest non-HLA

Table 1. Association Results and Meta-analysis of the Genome-Wide Association Studies and Replication Cohort for 5 Top Loci

		GWAS					Replication					Meta analysis[e]	
			RAF[b]				RAF[e]						
Location	SNP (candidate gene)	$N_{cases+controls}$[a]	Cases	Controls	OR (95% CI)[c]	P_{GWAS}	$N_{cases+controls}$[d]	Cases	Controls	OR (95% CI)[c]	P_{Repl}	$P_{Holm-corr}$[f]	$P_{GWAS+Repl}$[g]	P_{Het}[h]
6p21.3	*rs2187668 (HLA-DQA1)*	14079	0.32	0.15	2.9 (2.6–3.4)	1.2×10^{-48}	4552	0.27	0.13	2.5 (2.2–3.0)	1.0×10^{-31}	5.0×10^{-31}	1.5×10^{-78}	.9
12q24	*rs3184504 (SH2B3)*	14075	0.53	0.43	1.4 (1.2–1.6)	5.0×10^{-7}	4552	0.55	0.51	1.2 (1.0–1.4)	.02	.08	7.7×10^{-8}	.2
22q13.1	*rs6000782 (CARD10)*	14082	0.08	0.04	1.7 (1.4–2.1)	1.8×10^{-5}	4530	0.06	0.05	1.4 (1.0–1.8)	.03	.09	3.0×10^{-6}	.3
4q25	*rs11943338 (DKK2)*	14080	0.86	0.82	1.5 (1.2–1.7)	4.6×10^{-5}	4519	0.82	0.81	1.0 (0.9–1.3)	.6	.8	4.3×10^{-4}	.03
5p15.3	*rs550167*	14084	0.22	0.19	1.4 (1.2–1.6)	5.6×10^{-5}	4537	0.17	0.18	0.9 (0.8–1.1)	.4	.8	9.2×10^{-3}	1.4×10^{-3}

NOTE. Association results of 5 top SNPs with a P value $<5.0 \times 10^{-5}$ in the GWAS analysis and available allele frequencies in the replication control cohort.
CI, confidence interval; RAF, risk allele frequency.
[a]Number of successfully genotyped individuals in the AIH-GWAS cohort consisting of 649 AIH patients and 13,436 controls.
[b]Risk allele frequencies were assessed on Illumina CytoSNP 12.0 platform.
[c]Odds ratio and 95% confidence interval.
[d]Number of successfully genotyped individuals in replication cohort consisting of 451 AIH patients and 4,103 controls.
[e]Risk allele frequencies were assessed by Taqman (cases) and Human Affymetrix 6.0 platform (controls).
[f]Adjusted P value using to Holm-Bonferroni correction ($\alpha = .05$).
[g]Weighted P value–based meta-analysis of discovery and replication results using METAL.
[h]P value for heterogeneity.

susceptibility marker was *rs3184504* in the Scr homology 2 adaptor protein 3 (*SH2B3*) gene on chromosome 12 (Table 1). These associations held even after AIH patients displaying overlap with PBC and PSC were excluded. *HLA-DRB1*0301* was associated with an earlier age of onset and higher immunoglobulin G levels at presentation; in contrast, *HLA-DRB1*0401* was associated with a later onset of disease. The presence of *rs3184504* was associated with concomitant autoimmune disease. A suggestive association of *rs6000782* on chromosome 22 may also implicate involvement of the caspase recruitment domain family member 10 (*CARD10*) in AIH. These findings confirm and establish previous findings in smaller patient populations and better define the role of HLA in the pathogenesis of type I AIH. Furthermore, this work identifies the first genetic locus for type I AIH outside the major histocompatibility complex and suggests that the genetic risk factors for type I AIH overlap with other immune-mediated diseases, including PBC and PSC.

See page 443; editorial on page 270.

EXPERT REVIEWS

Magnetic resonance enterography of Crohn's disease

Expert Rev. Gastroenterol. Hepatol. Early online, 1–9 (2014)

Makoto Naganuma*[1], Tadakazu Hisamatsu[2], Takanori Kanai[2] and Haruhiko Ogata[1]

[1]*Center for Diagnostic and Therapeutic Endoscopy, School of Medicine, Keio University, 35 Shinanomachi, Shinjuku-ku, Tokyo 160-8582, Japan*
[2]*Department of Gastroenterology and Hepatology, School of Medicine, Keio University, 35 Shinanomachi, Shinjuku-ku, Tokyo 160-8582, Japan*
**Author for correspondence:*
Tel.: +81 333 531 211
nagamakoto@z7.keio.jp

Magnetic resonance enterography (MRE) has been reported to be a useful modality for the evaluation of luminal inflammation and extraintestinal complications in Crohn's disease (CD). A recent study indicated that the diagnostic ability of MRE was comparable to the diagnostic ability of other devices, such as ileocolonoscopy. MRE can be performed repeatedly because there is no radiation exposure. Therefore, MRE is useful as a method of follow-up for younger patients with established CD. It is useful for evaluating the efficacy of medical treatments, such as biologics. MRE can detect small intestinal lesions even if the endoscope does not pass through the stenosis. The concerns of availability of expertise and the costs associated with MRE should be addressed so MRE can be widely used for CD patients in the near future.

KEYWORDS: Crohn's disease • diagnostic accuracy • endoscopic remission • enteroscopy • magnetic resonance enterography

Crohn's disease (CD) is an immune-mediated disease with abdominal symptoms that include diarrhea, abdominal pain and perianal fistulas. Inflammation in CD involves the entire gastrointestinal tract, especially the small intestine. Ileocolonoscopy is useful for detecting inflammation in the colon and the terminal ileum; however, this technique is unable to assess the mid-small intestine. More recently, novel technologies to enable inflammatory bowel disease diagnosis have been developed, such as capsule endoscopy (CE) and balloon-assisted enteroscopy (BAE). These technologies have been established as useful modalities for the diagnosis and assessment of disease extent and severity. However, CD lesions are typically transmural and lead to progressive damage and complications, such as fistulas and abscesses. Thus, cross-sectional imaging is critical for the assessment of CD lesions. Computed tomographic and magnetic resonance enterography (CTE and MRE) have been reported to be useful modalities for the evaluation of luminal inflammation and extraintestinal complications in CD. MRE can be performed without radiation exposure, making it the preferred imaging technique for the evaluation of CD in children and adolescents. In this article, we have reviewed recent trends and topics regarding MRE for patients with CD.

MRE protocol

In reviewing the diagnostic accuracy of MRE, we should note the heterogeneity of MR imaging protocols, such as the use of different MRI magnets (1.5 Tesla [1.5T] or 3 Tesla [3T]), enteral contrasts and preparations for bowel distention. The diagnostic accuracy might differ according to the protocol of MRE. The 3T magnet increases the signal-to-noise ratio and reduces the time of image acquisition compared with the 1.5T magnet [1]. The 3T MRI is superior to 1.5T for detecting ulcers, whereas 3T is as accurate as 1.5T in detecting bowel wall thickness, enhancement and fistulas.

MRE requires the administration of a large amount of contrast medium orally. Typically, transit to the right colon has been observed within at least 40–60 min [2]. A recent review stated that MRE performed 40 min after the ingestion of oral contrast material is practical for patients' compliance and for providing effective MRE imaging [3,4]. In the authors' institution, patients are typically ordered to ingest 1500 ml of polyethylene glycol within 60 min prior to scanning.

 10.1586/17474124.2014.939631 © 2014 Informa UK Ltd ISSN 1747-4124

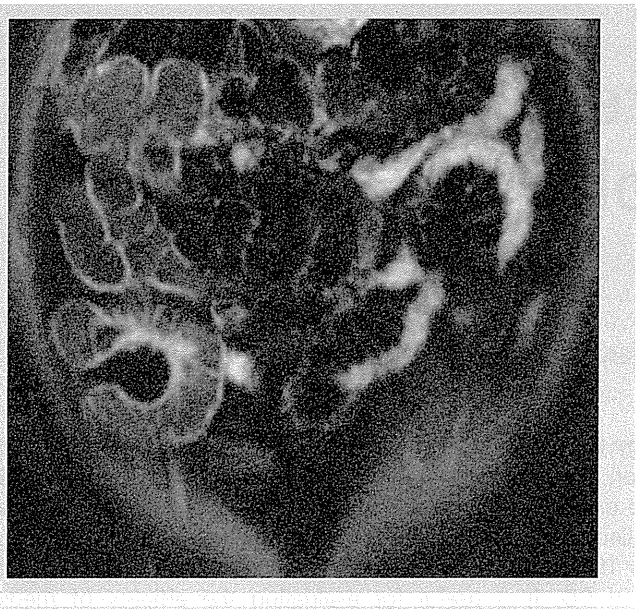

Figure 1. Coronal true imaging with T1-weighted images revealed that mural enhancement is observed in the proximal ileum after injection of gadolinium.

Bowel distention with MR enteroclysis is superior to distention with MRE in most studies [5–8]. However, the use of MRE is associated with reduced abdominal discomfort and nausea compared with MR enteroclysis. Patients are exposed to radiation during the placement of the naso-jejunal catheter when MR enteroclysis is performed [9]. Furthermore, a prospective randomized study showed that the diagnostic accuracy of MR enterography was comparable to the accuracy of MR enteroclysis [6,10]. Thus, MRE could be used to follow-up patients without proximal small intestinal lesions of CD [3].

Rectal contrast might increase the diagnostic accuracy in detecting lesions in the rectum and distal colon; however, rectal contrast causes more patient discomfort than MRE procedures done without using rectal contrast. For patients undergoing colonoscopy, the requirement for colonic distention during MRE is reduced [11]. Intravenous gadolinium chelate contrast agent is used to differentiate between active and inactive disease. Gadolinium chelate given to patients (approximately 60 s) prior to 3D T1-weighted image with fat suppression was acquired in the authors' institution.

The main limitation of MRE is bowel motion, which could potentially obscure relevant findings. Thus, anti-peristaltic agents such as scopolamine butylbromide or glucagon are used to minimize bowel motion just before MRE is performed. A recent study indicated that the quality of the MRE without anti-peristaltic agents was judged to be inferior to CTE, although the diagnostic results were equivalent [12]. The authors typically used anti-peristaltic agents for MRE to obtain high-quality imaging except in patients with contraindications for these agents.

Findings of MRE

The MRE findings for CD include wall thickness, wall hypersignal, extravascularity, swelling of lymph nodes, ulcerations, fistulas, edema, strictures and extraintestinal complications. In patients with active intestinal inflammation, mural enhancement is observed after the injection of gadolinium (Figure 1). Mural hyperenhancement is related to active inflammation and is the most sensitive finding of active CD lesions [3,13,14]. Wall thickness is also frequently observed; however, wall thickness without high intensity remains in responders after medical treatment in some cases (Figure 2).

Intestinal strictures can be detected on MRE. MRE enables the assessment of proximal small intestinal lesions beyond severe strictures even if the endoscope does not pass through the stenosis (Figure 3). This is the advantage of MRE for the assessment of intestinal lesions in patients with CD, compared with ileocolonoscopy and BAE. Moreover, while BAE has been available for evaluating small intestinal lesions of CD, it is hard to observe the mucosa along the entire length of the small intestine using either the oral or anal approach in one session of BAE. Intestinal strictures with marked intestinal distension suggest moderate-to-severe strictures, resulting in indications for surgery if the patients have any abdominal symptoms. Strictures with hypoenhancement are typically observed in fibrotic strictures, whereas inflammatory strictures have wall thickness with mural hyperenhancement and edema [15]. However, it is not easy to distinguish fibrotic strictures from inflammatory strictures on MRE in some cases, because the strictures are usually constructed of both fibrotic and inflammatory lesions.

Fistulas could be detected on MRE (Figure 4), although early fistulas might be difficult to detect because of the lower spatial resolution of MRE.

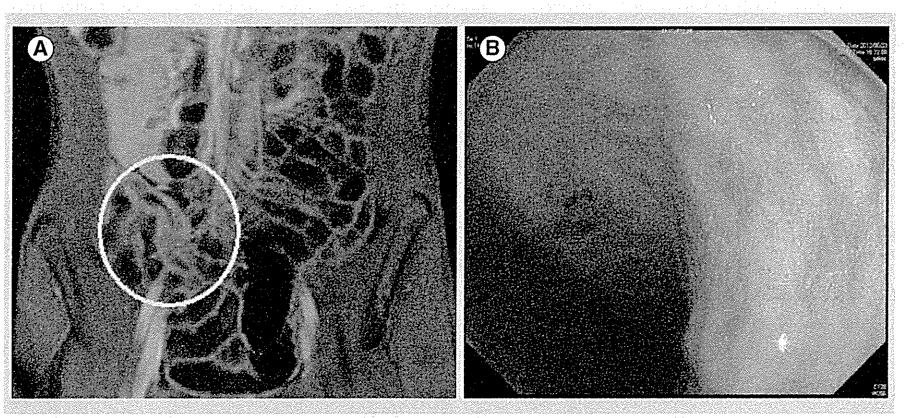

Figure 2. Comparison between ileal lesion on MRE and endoscopic finding.
(A) Increased wall thickness was observed at the terminal ileum. However, mural and transmural enhancement is minimal. **(B)** The endoscopic findings revealed no inflammation at same area.